J. Fluid Mech. (1991), *vol.* 225, *pp.* 497–528
Printed in Great Britain

Similarity and asymptotic analysis for gun-firing aerodynamics

By A. MERLEN AND A. DYMENT
ONERA-IMFL, 5 Boulevard Painlevé, 59000 Lille, France

(Received 27 November 1989 and in revised form 27 September 1990)

An experimental observation of the flow following the discharge of firearms has been carried out by means of ultra-high-speed visualization. The theory of similarity has been applied in order to define the rules governing the tests on models, chiefly for gun firing-air intake interference problems. When the blast effect predominates, no geometric similarity is required between the simulation gun and the simulated one, so the model and the simulation gun can have different scales. It is shown that the main parameter characterizing the blast effect is the energy rate at the muzzle which can be considered as a point source of energy caused by a very hot gas. So, the muzzle wave tends asymptotically toward the blast wave of a non-instantaneous intense point explosion. Specific experiments confirm this assertion. All previous results allow a theoretical modelling of gun-firing aerodynamic phenomena which will be presented in a separate paper.

1. Introduction

The discharge of firearms has spawned a great deal of research since Mach and Hugoniot, yet general works on the subject are scarce because of the complexity and variety of the phenomena following the firing.

In this paper, we are attempting to look at those aspects of firing a gun that are of interest to the aerodynamicist; namely the blast. The phenomenon of 'intermediate ballistics' does not in fact seem to have been scrutinized very closely from the fluid mechanics viewpoint. It is doubtless the often confidential nature of the research on weapon firing that has narrowed our thinking on the subject down to the specific technical problems of ballistics experts. But it should be added that the brevity of the phenomenon also calls for experimental means that are not commonly found in aerodynamics laboratories. It is precisely because we have such means that we were able to address this subject with a two-fold purpose. First, we wanted to use the combined power of our experimental and theoretical means to understand and quantify these phenomena. Secondly, we wanted to arrive at practical results that could be put to use, chiefly for guns on military aircraft. The prime objective here is the establishment of a rule of similarity for tests using models.

On the experimental level, we made abundant use of an ultra-high-speed visualization technique (figure 1).

On the theoretical level, we established and analysed the rules of similarity specific to the phenomenon and then, simplifying, we proposed a mathematical modelling of the firing process, based on the theory of intense explosions (Merlen 1988).

In this paper, we will speak only of that part of our research that relates to similarity, and we will justify the choice of the mathematical model. The mathematical developments will be presented in a separate publication.

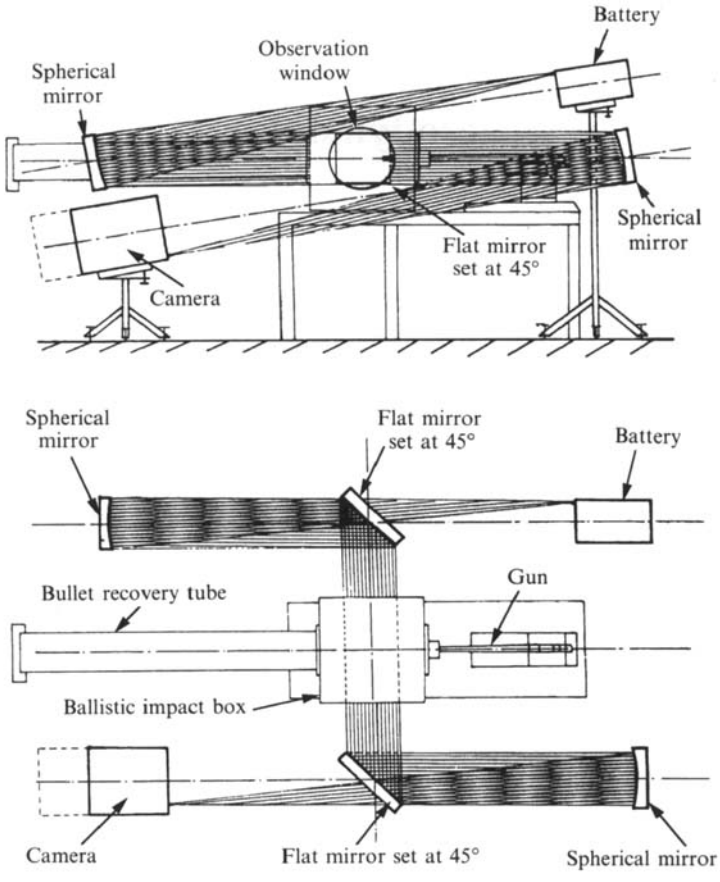

FIGURE 1. Cranz–Schardin ultra-high-speed visualization system which provides 24 shadowgraphs in succession. The flash duration is 200 ns and the time interval Δt is adjustable from 100 ns to 1 s.

2. Shooting in an infinite atmosphere

2.1. *Description of the phenomenon*

The visualizations of figure 2 are for a 5.56 mm calibre gun. This in no way restricts the generality of the following description, which remains valid for most long-barrel firearms propelling projectiles at speeds that are supersonic with respect to the exterior medium (Oswatitsch 1964; Schmidt & Shear 1975).

Subsequent to the firing, the burning of the powder produces a fast rise in pressure that sets the projectile into motion. The bullet compresses the air in front of it in the barrel, which therefore behaves much like a one-dimensional shock tube.

Many experiments (Mach *et al.* 1977; Fuller 1980; Merlen & Desse 1983) have shown that the projectile reaches a constant velocity V_p once it has travelled about a third of the barrel length. So we can get a good idea of how the 'plug' of air preceding the projectile in the barrel behaves, by assuming that it follows one-dimensional shock-tube theory in the limiting case where the projectile reaches its speed instantaneously. We then demonstrated (Merlen 1988) that this flow is supersonic for $\gamma = 1.4$ if V_p is greater than 1.33 times the velocity of sound in the external medium. This condition is largely verified for common firearms.

The shock formed in the driven air is called the precursor. Since the airflow is

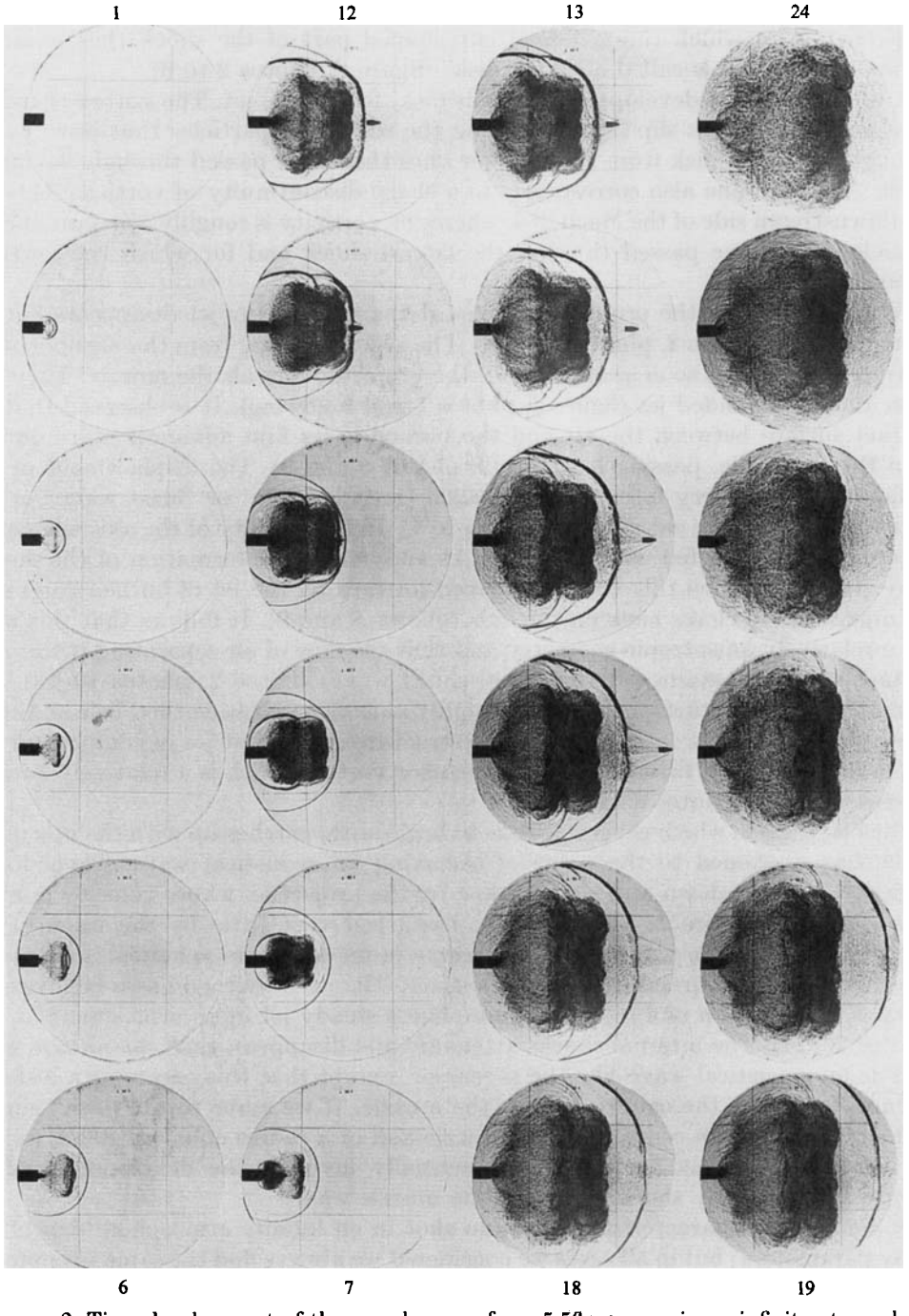

FIGURE 2. Time development of the muzzle wave for a 5.56 mm gun in an infinite atmosphere obtained with $\Delta t = 20\ \mu s$. The number of each picture indicates the sequential order.

supersonic, this shock has no reflection at the muzzle and the air compressed by the precursor expands outside the barrel. Because of the high level of pressure in the tube, the expansion is very intense and the boundaries of the jet are highly divergent. The characteristics that reflect at the boundary of the jet converge and form a shock

wave that cannot have a regular reflection on the axis. We then observe a Mach phenomenon in which the spherical cup-shaped part of the shock that is almost normal to the axis is called a 'Mach disk' (figure 2, photos 2 to 6).

A toroidal vortex develops around this disk, fed by the jet. The vortex is created by the existence of a slip line separating the slow fluid particles that have passed through the Mach disk from those faster ones that have passed through the lateral shock. This slip line also corresponds to a sharp discontinuity of vorticity between the downstream side of the Mach disk where the vorticity is roughly constant and the particles that have passed through the lateral shock and for which the vorticity varies continuously.

When the nose of the projectile arrives at the muzzle, the jet disappears but the vortex persists (figure 2, photos 5 and 6). The gases resulting from the burning of the powder spurt out as soon as the base of the projectile unseals the muzzle. They also form an overexpanded jet (figure 2, photos 7 and following). It is observed that the contact surface between the air and the burned gases first advances more quickly than the projectile, passing it (figure 2, photos 8 and 9). The displacement of this surface sets up a very intense shock called 'muzzle wave' or 'blast wave', which begins to form on the sides of the jet (photo 7). In the vicinity of the axis the vortex of compressed air is fed with burned gases and delays the formation of the muzzle wave. It is only when this vortex is driven forward by the jet of burned gases that the muzzle wave closes back on the axis (photos 8 and 9). It follows that this wave has a relatively anisotropic geometry and that the flow of air separating it from the contact surface contains some internal shock waves (figure 2, photos 10–18). The geometry of the contact surface is also highly anisotropic. Inside this surface, the jet of burned gases tends to adopt the same structure as the first jet of compressed air; but to do so, it must first absorb the precursor vortex, which is a relatively lengthy process (figure 2, photos 8 to 21).

The blast wave, which is very intense to begin with, catches up with the precursor, which has weakened to the point of becoming an acoustical wave. Then, losing intensity, it slows down and is overtaken by the projectile, whose velocity remains constant at V_p (figure 2, photos 8–12). Disturbed very little by the wake of the projectile, the muzzle wave tends to become more and more spherical as it moves away from the air-burned gas contact surface. The jet of burned gases behaves less and less like a piston and more and more like a steady jet in an atmosphere at rest (photos 20–24). The internal shocks attenuate and disappear, then the muzzle wave ends as an acoustical wave like the precursor, except that this occurs at a distance of some 100 times the calibre D from the muzzle. If we agree to the term 'muzzle vicinity' for a sphere centred on the muzzle and of a radius equal to $100D$, we can say that the intermediate ballistics essentially involves the development of an intense and unsteady shock wave, i.e. the muzzle wave.

Of course, the characteristics of a gun shot in an infinite atmosphere depend on many parameters; but in all cases we considered we always find the same phenomena as described above. Only the relative intensities of the shocks and the characteristic durations of each phase may change.

But a few parasitic phenomena may occasionally come into play, such as the appearance of a second precursor owing to a leakage of powder gases around the projectile as it advances through the gun tube.

When it exists, the main effect of this leak jet, beyond the fact that it creates a second precursor, is to reinforce the toroidal vortex due to the jet of the first precursor. This affects the time that the muzzle wave will take to close back on the

FIGURE 3. Time development of the muzzle wave for a 5.56 mm gun in presence of a two-dimensional air intake with $\Delta t = 20\ \mu$s between photographs. The air intake is fed by a uniform flow at $\bar{V} = 198$ m/s coming from the left. The projectile velocity is $V_p = 940$ m/s.

axis. The muzzle wave has more time to develop laterally before closing than in the usual case of figure 2. The result is that the muzzle wave takes the shape of a pear. As will be seen later, it is not necessary to establish any similarity rule concerning the leak jet.

Figure 2 shows that the projectile has little effect on the development of the muzzle wave: it does not delay its formation since the burned gases have no trouble getting around it, and it does not create any major disturbances either when it passes through the wave, or with its wake. So, the projectile constitutes a small disturbance for the muzzle wave, but one that is local and that cannot modify the blast effect in any global or durable way. It is therefore reasonable to think that a theoretical modelling of the blast effect could overlook the projectile.

The muzzle shock wave is very intense to start out with. So a body placed in the vicinity of the muzzle is subject to forces that are as intense as they are brief, and the body profoundly modifies the flow. As an example, we present in figure 3 the interaction between the shooting of a 5.56 mm calibre rifle and a two-dimensional subsonic flow over a schematic air intake formed by a plate parallel to the wall.

The presence of the body destroys the axisymmetrical character of the shot as soon as the precursor has reached the outer wall of the air intake (figure 3, photo 2). Observing the jet of burned gases from shadowgraphs 8–24, we see that it has evolved little, which leads us to think that its behaviour is quasi-steady throughout the process. On the last photos we can see that the burned gases have entered the air intake. We also observe reflection of the muzzle wave on the inner wall of the test section.

Analysing such a phenomenon is understandably very tricky, even with such precise visualizations. The problem is even knottier for large-calibre firing or for flight tests, for which experimental facilities are lacking. So it is natural to lean on the resources of physical similarity in this research. First, this makes it possible to concentrate on the shooting of small-calibre weapons, which lend themselves better to the visualizations, rather than going into all possible weapons. Secondly, it provides a method of phenomenological analysis. Finally, it yields the form of the laws relating the physical conditions to the sequence of events.

However, these laws can be completely determined only by calculation. The complexity of the flow therefore demands a mathematical modelling to trim the volume of numerical calculations down to size. Both the similarity and the modelling require a simplification of the physics of this phenomenon.

2.2. *Ideal firing*

We have seen that, from the aerodynamic point of view, the muzzle wave is the dominant phenomenon in the firing process. It is therefore reasonable to imagine an ideal firing, in which all precursor phenomena are done away with. This would be a shot in which the blast wave is pure, i.e. entirely determined by the properties of the jet of powder gases. Such a shot can be managed experimentally by getting rid of all of the physical causes of the precursor phenomena. Since the first precursor and its jet consist of a draining of the air out of the gun barrel, all we have to do to suppress them is to create a vacuum in the barrel before the shot is fired. To do this, the barrel is closed off by a membrane (which the projectile destroys in its passage), and the trapped air is drawn out before the shot (Schmidt, Gion & Fansler 1980). We avoid the second precursor by choosing a weapon for which there is no burned gas leakage.

Figure 4 is a visualization of this ideal firing, performed by a 7.62 mm calibre gun, under standard pressure and temperature conditions and in the absence of any body or counter flow. It is remarkable to observe that the ideal muzzle wave is quasi-spherical, despite the obvious anisotropy of the flow that creates it. This confirms that the precursor phenomena do originate the anisotropic forms observed in conventional firings in an infinite atmosphere. We also see that the projectile has

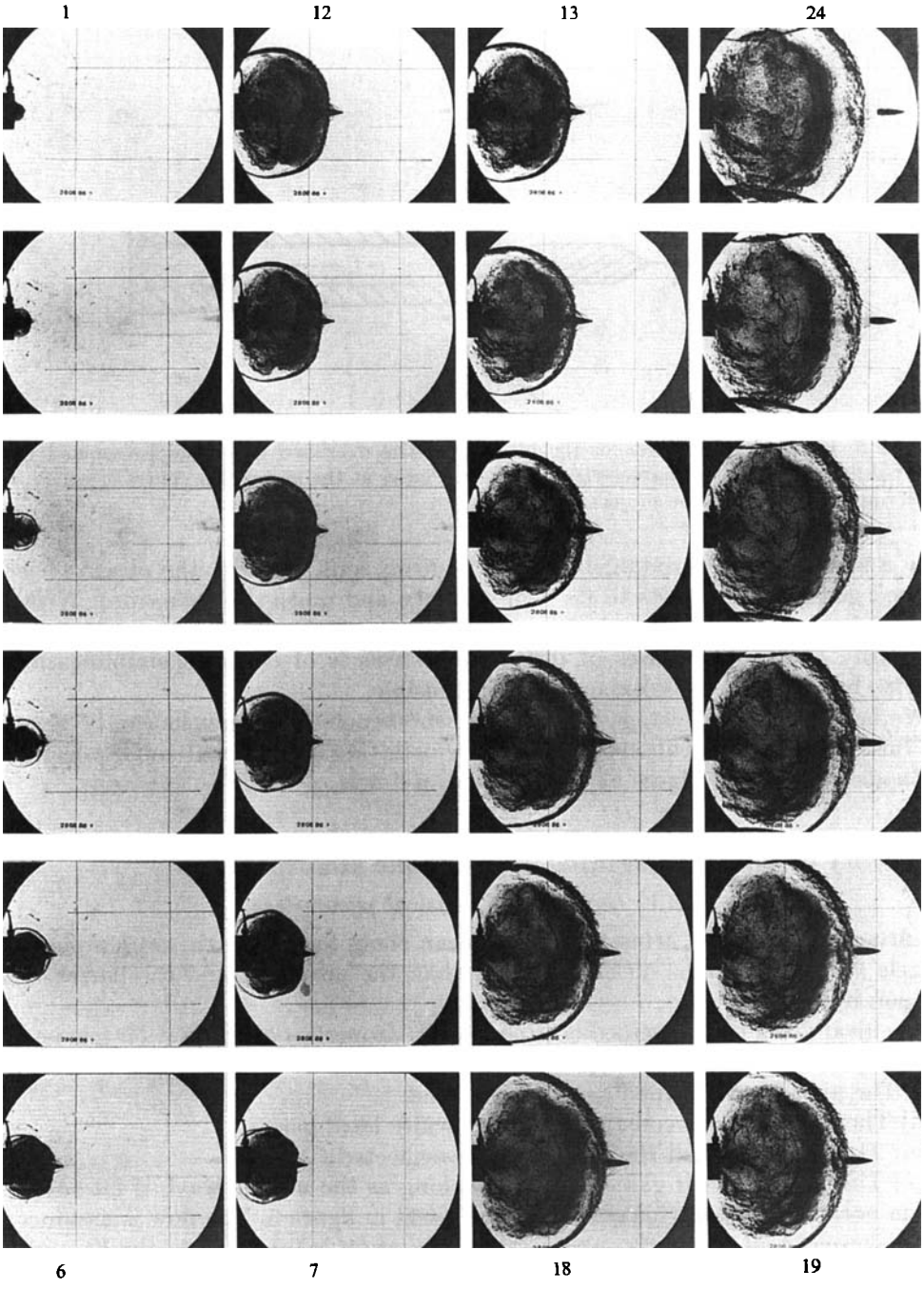

FIGURE 4. Ideal shoot for a 7.62 mm gun observed with $\Delta t = 20\ \mu$s. Precursor phenomena are avoided by closing the barrel with a membrane and drawing out the air trapped inside. There is no burned gas leakage and consequently no second precursor. The blast wave forms earlier than in figure 2 and its shape is almost spherical.

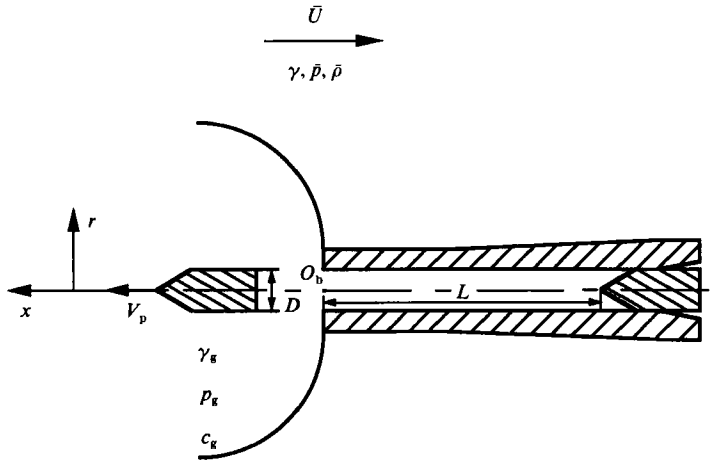

FIGURE 5. Physical parameters for the ideal shot. The overlined quantities correspond to the external flow. Subscript g characterizes the burned gases at the muzzle the centre of which is O_b. Subscript p is related to the projectile.

only a small and localized effect along the firing axis. Finally, the observed jet of burned gases again attests to its own stability and quasi-steady nature. With the ideal firing, we have isolated the preponderant phenomenon by eliminating the ordinarily observable causes of disturbance. This is of course a simplification of reality, but the scheme is experimentally feasible.

We have reached the stage where the phenomenological analysis can be brought no further by simple observation. Henceforth, we must avail ourselves of the methods that theory places at our disposal, the first of which is similarity.

3. Theory of similarity of firing in an infinite atmosphere

3.1. *Inventory of physical parameters*

By firing in an infinite atmosphere, we mean shots for which the area around the muzzle vicinity contains no bodies other than the projectile and the barrel of the weapon itself.

The ideal firing is determined entirely by the properties of the powder gas jet. We will adopt the following assumptions.

(i) The air and the burned gases are inviscid.

(ii) The burned gases constitute a calorifically ideal gas.

(iii) The projectile and the barrel can be neglected.

(iv) The jet of burned gases is steady as long as the muzzle wave is intense.

The notation used in this section is explained in figure 5. The flow is assumed to be axisymmetrical about the x-axis. The time origin is taken when the base of the projectile unseals the barrel.

It is obvious that, in dealing with the propagation of a shock, it is legitimate to neglect the viscosity. But can we get around the thermodynamic problems of the powder gases as easily as that? Hypothesis (ii), according to which the burned gases constitute an ideal gas, is equivalent to considering them as fixed in their composition. It has been proven in Dyment & Merlen (1981) that all of the conclusions reached under the ideal gas hypothesis are conserved along with the hypothesis of chemical equilibrium on condition that γ_g be replaced by a set of five

thermochemical parameters. We will see in §4.1 that, within the bounds of the cases studied, the temperature at the muzzle is less than the freeze temperature measured in a calorimetric bomb. Moreover, as the composition of the powder gases varies little from one gun to another, we will consider that the ratio of the speeds of sound at the muzzle of a gun of calibre D with respect to a gun of calibre D' is connected to the temperature ratio by:

$$\frac{c'_g}{c_g} = \left(\frac{T'_g}{T_g}\right)^{\frac{1}{2}}.$$

The pertinence of hypothesis (iii) derives from the observation described in §2. At this stage in the simplification, the muzzle is likened to an extensive source of mass, momentum and energy, and of diameter D.

Hypothesis (iv) is based not only on the observation of ultra-high-speed visualizations, but also on muzzle pressure and temperature measurements (figures 6 and 7, §4.1).

This hypothesis, surprising as it may be for a ballistics expert, for whom the characteristic times of a shot are of the order of the path of the projectile, is justifiable according to interior ballistic considerations (Merlen 1988). Without going into the detail on this, we may quickly indicate the reason for this behaviour. When its base reaches the muzzle, the projectile is, depending on the gun, either subsonic or supersonic with respect to the burned gases. If it is subsonic, a sonic throat is set up at the muzzle as soon as the base of the projectile passes, because of the external expansion. If it is supersonic, there necessarily exists a sonic section advancing through the tube behind the base. This section reaches the muzzle shortly after the base, and does so all the more quickly the closer the projectile velocity V_p is to c_g. As soon as this section reaches the muzzle, we again find the sonic throat. So, at the muzzle, after a brief unsteady phase, we have $M_g = 1$ and, since the pressure and temperature are very high in the barrel, this blockage of the flow constitutes a break to the draining process and consequently imposes a very slow variation on p_g and T_g.

With all our hypotheses, we can express the mass, momentum and energy rates at the muzzle by:

$$\left.\begin{aligned}
&\rho_g c_g M_g \frac{\pi D^2}{4} = \gamma_g \frac{p_g}{c_g} M_g \frac{\pi D^2}{4}, \\
&(\rho_g c_g^2 M_g^2 + p_g)\frac{\pi D^2}{4} = (\gamma_g M_g^2 + 1)\, p_g \frac{\pi D^2}{4}, \\
&\left(\frac{\gamma_g p_g}{(\gamma_g - 1)\rho_g} + \tfrac{1}{2} c_g M_g^2\right)\rho_g c_g M_g \frac{\pi D^2}{4} = \frac{2 + (\gamma_g - 1) M_g^2}{2(\gamma_g - 1)} \gamma_g p_g c_g M_g \frac{\pi D^2}{4}.
\end{aligned}\right\} \qquad (1)$$

So, the weapon is characterized by D and by the flow rates (1), which depend only on the quantities γ_g, M_g, c_g and $p_g D^2$. We can replace these quantities by $\mathscr{P} = c_g p_g D^2$ and $\mathscr{Q} = (p_g/c_g) D^2$, representing the power and mass flow rate of the firing.

The external environment is characterized by γ, its velocity $\bar{U}$, density $\bar{\rho}$ and pressure $\bar{p}$. That leads to the following inventory for the ideal firing:

$$\gamma,\ \bar{U},\ \bar{\rho},\ \bar{p},\ \gamma_g,\ M_g,\ \mathscr{P},\ \mathscr{Q},\ D. \qquad (2)$$

Usually, the gun firing is not ideal and we will use the term 'formation phase' to designate the period of time during which the precursor phenomena and nascent muzzle wave interact. To simplify, we assume that there is no second precursor. We will see in §4.5 that we can also simulate the two-precursor case with this approach.

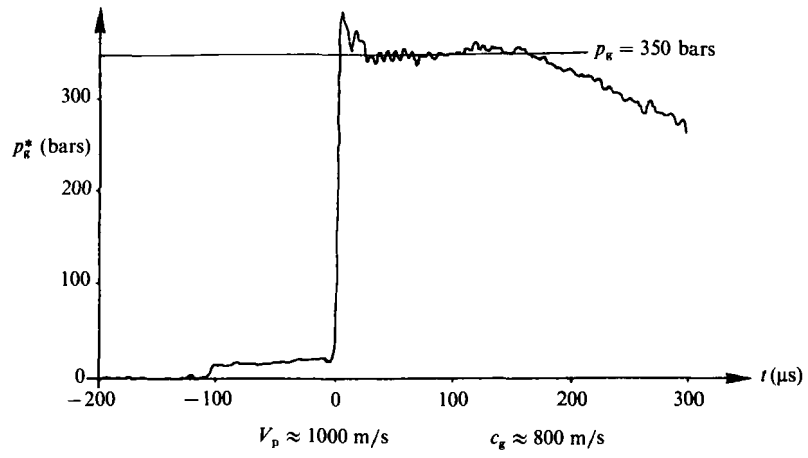

FIGURE 6. Muzzle pressure measurement for a 5.56 mm gun. After a short fluctuation, the pressure stabilizes during a period of time which corresponds to the intense phase of the blast wave development. The sound velocity at the muzzle is about 800 m/s.

The formation phase in an infinite atmosphere is determined uniquely by the draining of the air out of the gun barrel. We can consider this draining to be a uniform supersonic flow because the projectile reaches its final velocity V_p very quickly. So between the passage of the precursor and the arrival of the projectile, the fluxes at the muzzle are given by:

$$\left.\begin{aligned} &\gamma \frac{p_T}{c_T} M_T \frac{\pi D^2}{4}, \\ &(\gamma M_T^2 + 1) p_T \frac{\pi D^2}{4}, \\ &\frac{2+(\gamma-1)M_T^2}{2(\gamma-1)} \gamma p_T c_T M_T \frac{\pi D^2}{4}, \end{aligned}\right\} \tag{3}$$

in which p_T, c_T and M_T are respectively the pressure, speed of sound and Mach number in the gun barrel behind the precursor. Three new quantities now appear for consideration: $p_T D^2$, c_T and M_T. Let $\overline{p_T}$ and $\overline{c_T}$ be the pressure and speed of sound in the barrel before the precursor passes. The pressure $\overline{p_T}$ is equal to $\bar{p}$ if the external medium is at rest; but if there is a counterflow, it is equal to the stagnation pressure of the outer flow. The same remark applies to $\overline{c_T}$. We can, however, set $\overline{p_T}$ independently of any counterflow by closing the barrel with a membrane which is destroyed when the projectile passes through. Then $\overline{c_T}$ is equal to $\bar{c}$.

It is clear that $p_T D^2$, c_T and M_T are related to $\overline{p_T} D^2$, $\overline{c_T}$ and $\overline{M_{PT}} = V_P/\overline{c_T}$ by the normal shock laws. Moreover, $\overline{c_T}$ is equal to $\bar{c}$ (for the membrane case) or related to $\bar{c}$ and $\overline{M} = \bar{U}/\bar{c}$ by Hugoniot's relation. Since $\bar{c}$ and $\bar{U}$ are already taken into account in (2), the flow rates (3) introduce only two new quantities: $\overline{p_T} D^2$ and V_p.

To take the draining duration into account the internal length of the gun barrel L also has to be retained in the list.

In summary, the formation phase in an infinite atmosphere calls for introducing the following set:

$$V_p, \quad \overline{p_T} D^2, \quad L$$

We see here that two characteristic lengths of the weapon, the calibre D and the length of the barrel L, appear in the list. This raises a question of great practical interest: is there a degree of freedom between these two lengths? Or, in other words, is geometric similarity necessary for the weapon?

To answer this question we must use the principles of physical similarity and compare the resulting dimensionless parameters.

3.2. *Similarity rules*

The physical parameters can be listed as follows:

$$\gamma, \bar{U}, \bar{\rho}, \bar{p}, \tag{4}$$

for the external environment,

$$\gamma_g, M_g, \mathscr{P}, \mathscr{Q}, D, \tag{5}$$

for the jet of burned gases,

$$M_p = \frac{V_p}{\bar{c}}, \quad \overline{p_T} D^2, \quad L, \tag{6}$$

for the formation phase.

In order to apply the principles of similarity in mechanics, we have to choose a set of three primary or reference quantities (Sedov 1959). Formally, this choice has no importance since all the quantities included in the inventory appear in the dimensionless parameters. Nevertheless, some choices are better than others if the purpose is to eliminate the less relevant dimensionless parameters. Of course, only a perfect knowledge of the phenomenon allows us to choose the most accurate primary quantities system. At this stage of the paper, it is premature to discuss it. So, without any restriction of generality, we will take the following set:

$$\bar{\rho}, \bar{p}, \mathscr{P}. \tag{7}$$

The following sections will reveal this choice to be best suited to the phenomenon. Chiefly, it provides a way of studying its asymptotic behaviour as will be seen in §6.

Any local quantity in the flow depends on the parameters (4), (5) and (6), on the coordinates x_i and on the time t. By writing the dimensionless formulae using the quantities of (7), we get, for any local quantity such as the pressure, an expression of the form:

$$\frac{p}{\bar{p}} = \mathscr{F}_D\left[\gamma, \gamma_g, M_g, \bar{M}, \frac{\bar{p}\mathscr{Q}}{\bar{\rho}\mathscr{P}}, M_p, \left(\frac{\bar{p}^3}{\bar{\rho}\mathscr{P}^2}\right)^{\frac{1}{4}} L, \left(\frac{\overline{p_T} D^2}{\mathscr{P}}\right)\left(\frac{\bar{p}}{\bar{\rho}}\right)^{\frac{1}{2}}, \left(\frac{\bar{p}^3}{\bar{\rho}\mathscr{P}^2}\right)^{\frac{1}{4}} D, \left(\frac{\bar{p}^3}{\bar{\rho}\mathscr{P}^2}\right)^{\frac{1}{4}} x_i, \left(\frac{\bar{p}^5}{\bar{\rho}^3\mathscr{P}^2}\right)^{\frac{1}{4}} t\right],$$

in which $\mathscr{F}_D$ is a universal function characteristic of a weapon fired in an infinite atmosphere.

Unsteady pressures are difficult to measure in an infinite atmosphere; but the position of the muzzle wave can be determined by ultra-high-speed visualizations. This position X on the firing axis can be expressed in dimensionless quantities, and using the expression for $\mathscr{P}$ and $\mathscr{Q}$ as a function of p_g and c_g, we get:

$$\mathscr{I}\frac{X}{D} = \chi_D\left(\gamma, \gamma_g, M_g, \bar{M}, M_p, \frac{\bar{c}^2}{c_g^2}, \mathscr{I}\frac{L}{D}, \frac{\overline{p_T} c}{p_g c_g}, \mathscr{I}, \mathscr{I}\frac{\bar{c}t}{D}\right), \tag{8}$$

where

$$\mathscr{I} = \left(\frac{\bar{p}}{p_g}\right)^{\frac{1}{2}}\left(\frac{\bar{c}}{c_g}\right)^{\frac{1}{2}}. \tag{9}$$

We notice here the unexpected fact that the dimensionless parameter corresponding to D is $\mathscr{I}$ which does not depend on D. This point will be clarified in §6.

Similarity exists between two shots from firearms of calibres D and D' if the following conditions are met:

$$\gamma = \gamma', \quad \gamma_g = \gamma'_g, \quad \bar{M} = \bar{M}', \quad M_g = M'_g, \tag{10a–d}$$

$$\mathscr{I} = \mathscr{I}', \quad \frac{\bar{c}^2}{c_g^2} = \frac{c'^2}{c'^2_g}; \tag{11a, b}$$

$$M_p = M'_p, \quad \mathscr{I}\frac{L}{D} = \mathscr{I}'\frac{L'}{D'}, \quad \frac{\overline{p_T c}}{p_g c_g} = \frac{\overline{p'_T c'}}{p'_g c'_g}. \tag{12a–c}$$

The conditions (10) and (11) are for an ideal firing. Condition (12) characterizes the formation phase. Of course, the forms (11) and (12) simplify and lead to the very strict conditions:

$$\frac{\bar{p}}{p_g} = \frac{\bar{p}'}{p'_g}, \quad \frac{\bar{c}}{c_g} = \frac{\bar{c}'}{c'_g}, \quad M_p = M'_p, \quad \frac{L}{D} = \frac{L'}{D'}, \quad \frac{\bar{p}_T}{p_g} = \frac{\bar{p}'_T}{p'_g}. \tag{13}$$

In practice, these conditions generally lead to the identity $D = D'$. As often happens, a poor simplification of the phenomenon results in conditions that are impossible to realize on small-scale models. This is why we broke the ideal firing conditions down into two sets, with (10) containing parameters of the order of unity and (11) parameters that are small compared to unity. The experimental procedure we followed is based on this classification. We attempted to bring out any asymptotic properties there may be, by allowing the small parameters to approach zero as far as possible. We shall see that formula (8) can exhibit asymptotic limits of the first kind, i.e. in such a way that a limit exists when the small parameters tend towards zero independently (Barenblatt 1979).

4. Experimental verification of the theory

4.1. *Test facilities and special measurement methods*

To verify the theoretical results of similarity, firing must be made under a variety of different physical conditions, but in compliance with the invariance of the similarity parameters. We then measure the values taken by the necessary number of physical quantities and form the corresponding dimensionless groups using the chosen primary quantities. The similarity is verified if the values of these dimensionless groups coincide at the homologous points and times defined by:

$$\mathscr{I}\frac{x_i}{D} = \mathscr{I}'\frac{x'_i}{D'}, \quad \mathscr{I}\frac{\bar{c}t}{D} = \mathscr{I}'\frac{\bar{c}'t'}{D'} \tag{14}$$

Conditions (10) and (11) depend on the characteristics of the ammunition and of the exterior atmosphere. We made different weapons and, to cover a greater range of variations in the similarity parameters, we designed a test facility for firing shots of small calibre in a controlled atmosphere. The pressure $\bar{p}$ and temperature $\bar{T}$ can be adjusted to provide the dimensionless parameters (10) and (12) with the desired values. As there is no need to represent a flow in the facility to study the firing itself, $\bar{U}$ will be left at zero.

The experimental device consists of a sealed, thermally insulated cubic box, of edge 400 mm. The projectile is recovered from the end of a tube welded on the box. Only the end of the gun barrel extends into the box, the upper wall of which supports a liquid nitrogen spray capable of cooling the inside of the test device to 223 °K, to reproduce the variations of $\bar{T}$ in the atmosphere. To avoid any condensation, liquid

nitrogen is injected after the box is evacuated. The nitrogen vaporizes and the pressure $\bar{p}$ is adjusted in the box by a vacuum pump. An oxygen input is used to reconstitute a mixture of gases similar to that of air. A high-precision pressure gauge measures $\bar{p}$, which can be adjusted continuously from 1 to 0.1 bar. The temperature $\bar{T}$ is measured by four thermocouples arranged in the field and verifying the temperature homogeneity of the medium.

The measurable quantities are the pressures on the bodies and the time advance of the muzzle wave. For the former, the box has measurement probes for unsteady pressure transducers. The latter is measured by the ultra-high-speed visualization system of figure 1. The lateral walls of the box are fitted with windows, so that the phenomenon can be visualized over a field 250 mm in diameter.

As for the 30 mm cannon, it has been tested in standard atmospheric conditions for obvious technical reasons.

The pressure p_g, which is indispensable for calculating the dimensionless parameters of (10)–(12), is measured by a piezocapacitive transducer installed flush inside the gun barrel, a few millimetres from the muzzle. Figure 6 shows the type of signal obtained. The various redundant measurement methods used to validate this technique, commonly used in interior ballistics laboratories, have been compared (Merlen 1988).

The temperature T_g is also a quantity affecting conditions (10)–(12) and relations (14), through c_g. A technique was developed at the Institute of Saint Louis (France) to measure this. The method is based on the measurement of the light emission and absorption in the burned gas jet. These optical properties of the jet are related to the temperature by Planck's law. Measurements are realized a few millimetres outside of the muzzle (Mach *et al.* 1977; Mach 1978; Eichhorn *et al.* 1984).

For all the guns used in this study we found muzzle temperatures clustered about 1400 °K on the firing axis, where the effect of the outer expansion is lesser. Figure 7 shows the results obtained for various guns. It can be seen that the time variation is slow, which confirms the hypothesis of the steady jet and sonic muzzle conditions according to §3.1. So, in the whole study, condition (10*d*) always holds with $M_g = 1$.

More than 500 weapons of different calibres were used in this research. It is obviously impossible to present all the results, firstly because our aim is to insist on the main facts excluding irrelevant details, but also because of a presentation problem. As a matter of fact, it is well known that similar phenomena follow the same dimensionless law, so, in a dimensionless representation like (8), it is impossible to detect any difference between two similar shots. If a dimensionless parameter is studied the effect of which is weak, it is very possible that this effect does not exceed the measurement errors. To avoid this drawback we chose to present in this paper only a few significant results.

4.2. *Thermochemical effects*

In the many tests conducted no effects have been detected in the quantities measurable by our techniques, i.e. chiefly p and X, that could be attributed to the type of powder being used. This is most probably due to the fact that the composition of the burned gases is always roughly the same. The variations in powder charge composition are important to the vigour of the shot, i.e. in the period during which the projectile reaches its velocity, which is well before the phenomena we are analysing.

We agreed, as is done in many articles to consider that all of the powders studied

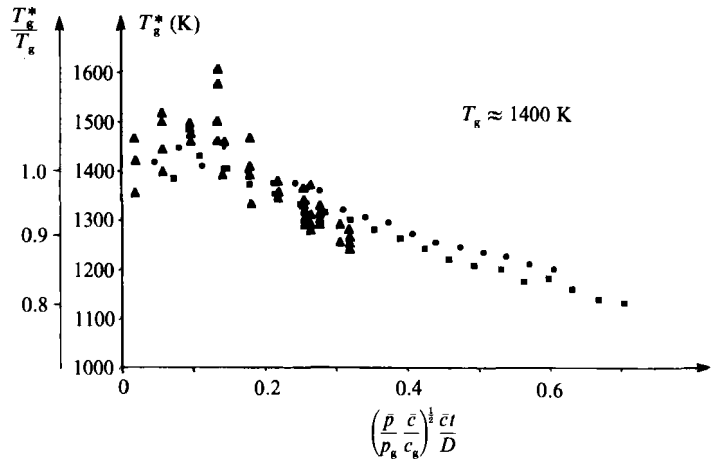

FIGURE 7. Muzzle temperature variation versus the dimensionless time for different weapons. The measurement is realized at 3 mm outside the muzzle. Taking into account the effect of the expansion, a value of 1400 °K at the muzzle has been estimated. ■, experimental weapon, $D = 5.56$ mm (double base powder); ●, gun, $D = 5.56$ mm (single bass powder); ▲, cannon, $D = 30$ mm.

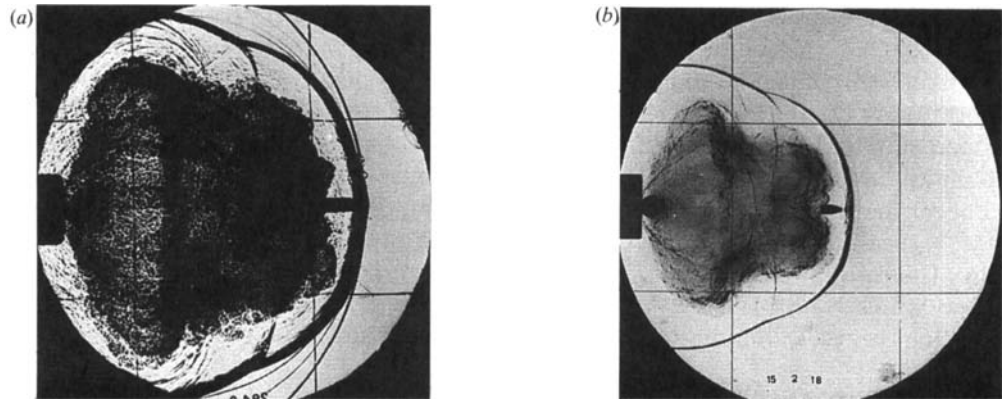

FIGURE 8. Blast waves produced by two weapons of different calibres: (*a*) 7.62 mm gun; (*b*) 5.56 mm gun. Similarity conditions hold except for a small variation of $\mathscr{I}(L/D)$ and $(\bar{c}/c_g)(p_T/p_g)$ which are respectively 3.26 and 1.510^{-3} in (*a*) and 3.3 and 1.310^{-3} in (*b*). This variation has no effect on the shape of the waves. No membrane was used in either case, so $\bar{p} = \overline{p_T}$. The atmosphere temperature is 288 °K. The mass of the 5.56 mm projectile is adjusted in order to realize the similarity on M_p ($M_p = 2.3$). Photographs (*a*) and (*b*) correspond to the same dimensionless time: $\mathscr{I}(\bar{c}t/D) = 0.3$.

produce an ideal gas that follows a polytrophic law of exponent $\gamma_g = 1.25$, having a number of moles per kg, $n = 46.6$. This conception is validated by tests on calorimetric bombs (Tavernier 1954), which indicate a powder gas freeze temperature of 1583 °K. Figure 7 shows that we are well within this value at the muzzle of the gun.

In order to illustrate our purpose, we present in figures 8 and 9 the comparison between a 5.56 mm calibre gun firing and a 7.62 mm one. The similarity conditions have been adjusted so that the firings only differ by the nature of the powder. In figure 8, we can see that the muzzle wave shapes are identical, as are the axial propagations in figure 9.

We may point out that the parameters $\mathscr{I}(L/D)$ and $\overline{p_T c}/p_g c_g$ were set rather

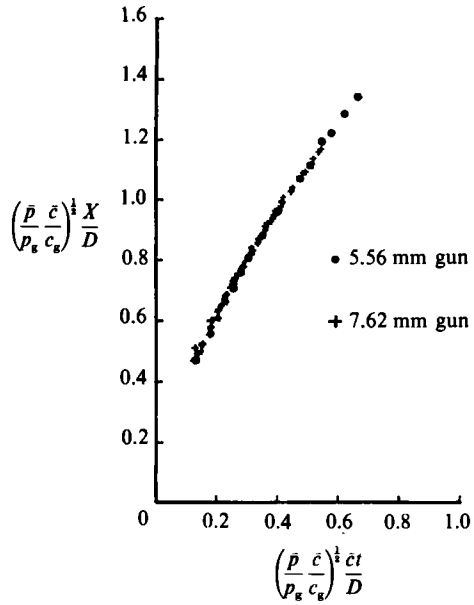

FIGURE 9. Axial propagation of the blast waves presented in figure 8. In dimensionless coordinates no difference appears between the two curves. The similarity on the shape allows us to conclude that similarity is realized on the blast waves propagation not only on the firing axis but also in every direction. ●, 5.56 mm gun; +, 7.62 mm gun.

approximately. However, the phenomenon is not affected by these slight variations. This remark will be very helpful hereafter, as it is technically very difficult to establish a perfect similarity on the basis of both (11) and (12) simultaneously.

4.3. *Effect of the source size*

Using the primary quantities of (7), the calibre D introduces the condition (11a), which leads to (13) and therefore, in practice, to the identity of the scales between the firearm being simulated and the one used to simulate it. To achieve a large variation in $\mathscr{I}$ we made use of the comparison between the firing of the 30 mm gun and that of a 5.56 mm rifle.

Figure 10 illustrates the waveforms obtained by complying with the conditions (12). This figure calls for a few remarks. First, the comparison with figure 8 constitutes a remarkable confirmation of the validity of the conditions (12): the same rifle (calibre 5.56 mm) was used in both tests, presented in figures 8 and 10. In the second case, to give the last parameter (12) the value corresponding to the cannon, a sealed membrane was set at the muzzle of the 5.56 mm calibre gun, and the barrel inflated at a pressure $\overline{p_T}$ greater than $\bar{p}$, which was determined to meet the second condition (12). It can be seen in figure 10, that the resulting modification in the waveform almost simulates that of the 30 mm gun, as the theory predicts. The remaining difference in the wave shape is caused by the effect of $\mathscr{I}$ which characterizes the source size (§3.2). Unfortunately a more accurate comparison of the waveform is difficult to make with our means. As a matter of fact, only a small portion of the 30 mm gun wave can be observed because the field visualized by the optical device cannot be enlarged. The lenticular shape of the image is explained by the absence of a box around the cannon. We also note that the projectile proportions do not comply with our modelling.

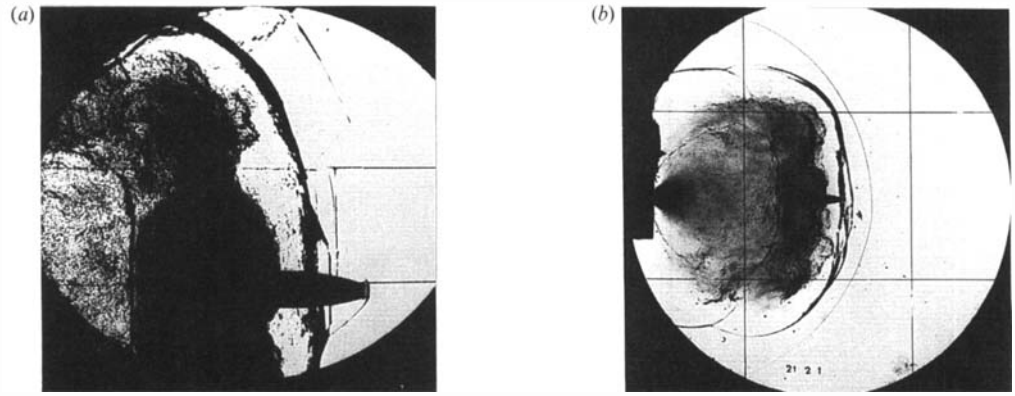

FIGURE 10. Blast waves produced by a 30 mm cannon (*a*) and a 5.56 mm gun (*b*). A membrane was used in firing (*b*) in order to adjust $(\bar{c}/c_g)(\overline{p_T}/p_g)$ which was 3.210^{-3} in both cases. Similarity conditions hold except on $\mathscr{I}$ ($\mathscr{I} = 5.5410^{-2}$ in (*a*) and 2.6910^{-2} in (*b*)). The pressure $\bar{p}$ is adjusted in the box to compensate the difference in p_g between the weapons. $M_p = 2.4$, $\mathscr{I}L/D = 2.58$ and $\mathscr{I}\bar{c}t/D \approx 0.25$. The length of the projectile is not similar as we assume in hypothesis (*c*). The waves are compared only at the beginning of their travels because the optical field cannot be enlarged enough to visualize the cannon wave later.

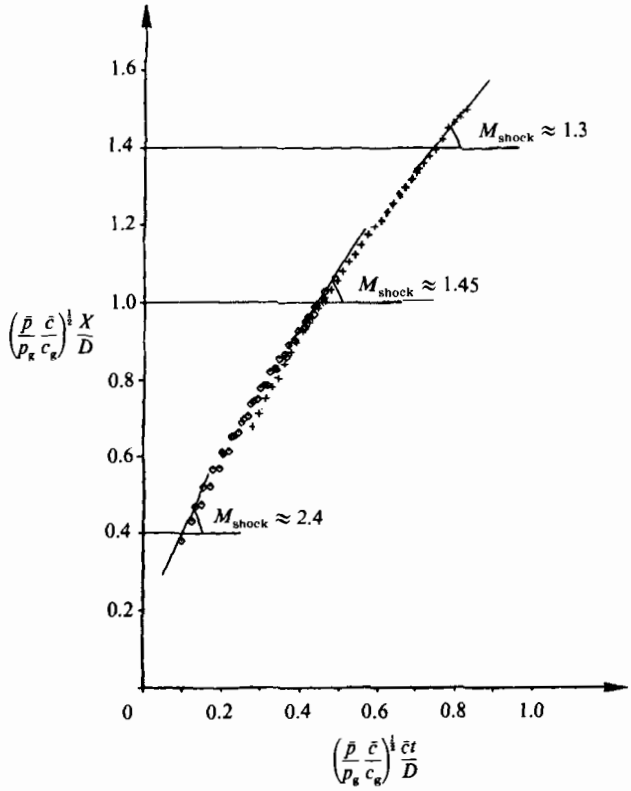

FIGURE 11. Axial propagations in dimensionless coordinates corresponding to the waves of figure 10. The slope of the curve is the Mach number of the blast wave. +, cannon; ◇, gun.

Figure 11 shows the corresponding axial propagations of the muzzle waves. We observe that the wave produced by the cannon forms further away from the muzzle and advances more quickly at the very beginning of its existence. Then, after moving far enough away, it adopts the same speed of propagation as the wave produced by the rifle. These differences in figures 10 and 11 may be due to the effect of $\mathscr{I}$, the only parameter whose value varies from one shot to another. This phenomenon can be interpreted as follows. When the projectile leaves the tube, the muzzle wave does not form instantaneously, even in the absence of any precursor phenomenon. During this lapse of time, the flow is not steady and therefore cannot follow the similarity rules established here for a steady jet. This phenomenon affects an area near the muzzle whose dimensions are of the order of D. On this scale, we cannot neglect the size of the source nor even of the projectile, whose interaction with the nascent jet is important. It is only after a long enough period of time ($\mathscr{I}(\bar{c}t/D) \sim 0.5$) and a great enough distance that these initial effects are no longer detectable. Figure 11 shows that the smaller $\mathscr{I}$ is, the sooner the muzzle wave forms. We may therefore say that the time it takes the muzzle wave to form increases with $\mathscr{I}$. So the question that should be asked is: does there exist an asymptotic behaviour of the muzzle wave as $\mathscr{I}$ tends toward zero? Experimentally, the condition

$$\mathscr{I} \ll 1, \tag{15}$$

is to be achieved, which is possible if $p_g \gg \bar{p}$, i.e. for an intense shot. We may note that, though this parameter can be assimilated to zero for a small enough value of $\mathscr{I}$, then this comes down to eliminating D from the parameter set (5). An infinitely intense shock then corresponds to a point source.

The limit case is the one where, in the absence of any precursor phenomenon, a muzzle wave formation phase is of zero duration. Figure 4, where $\mathscr{I}$ is equal to 3.5×10^{-2}, shows that for this low value of the parameter, the experiment is very close to such a limiting case. This suggests the existence of a finite function χ_0 as the limit of χ_D as $\mathscr{I}$ tends toward zero.

We will put off the theoretical discussion on the existence and consequences of this affirmation until §6; but let us now raise one experimental consequence related to the fact that $\mathscr{I}$ is never strictly zero.

It is obvious that replacing $\mathscr{I}$ by zero in χ_D is legitimate only if we do the same for any small parameters of the same order of magnitude, with respect to which the function is regular. This is precisely the case for $\mathscr{I}(\bar{c}t/D)$ at the beginning of the motion. So we can assimilate χ_D to χ_0 given by

$$\mathscr{I}\frac{X}{D} = \chi_0\left(\gamma, \gamma_g, M_g, \overline{M}, M_p, \frac{\bar{c}^2}{c_g^2}, \mathscr{I}\frac{L}{D}, \frac{\overline{p_T c}}{p_g c_g}, \mathscr{I}\frac{\bar{c}t}{D}\right), \tag{16}$$

only if

$$\mathscr{I}\frac{\bar{c}t}{D} \gg \mathscr{I},$$

i.e. if

$$\frac{\bar{c}t}{D} \gg 1, \tag{17}$$

and consequently in a domain where

$$\mathscr{I}\frac{x_i}{D} \gg \mathscr{I},$$

i.e.
$$\frac{x_i}{D} \gg 1. \tag{18}$$

If (15) holds, it is under the space and time conditions (17)–(18) that it is legitimate to neglect the size of the source.

It can be seen in figure 11 that the shock wave degenerates into an acoustic wave for $\mathscr{I}(x/D) \approx 2$. So, the intense phase of the blast wave can be observed only if $X \approx 2D/\mathscr{I}$ is sufficiently greater than the abscissa where the latter forms. The 30 mm cannon firing presented in figure 10 is the weakest (in the sense of (15)) that we studied, and we found the following results: the wave forms at $X \approx 12D$, $2.D/\mathscr{I} \approx 35D$ and the similarity with the 5.56 mm gun begins at $X \approx 16D$. Figure 11 illustrates this clearly. For most of the cases the wave forms before $X = 12D$, and $\mathscr{I}$ is generally smaller than 5×10^{-2}, so the blast wave does not degenerate before $X = 40D$. In any case, it is important to notice that the ratio of the duration of the formation phase to that of the intense phase only depends on $\mathscr{I}$ and not directly on D. These remarks allow us to give a more practical definition of (15), and (17)–(18):

$$\mathscr{I} \leqslant 5 \times 10^{-2}, \tag{19}$$

$$\frac{\bar{c}t}{D} \geqslant 5, \tag{20}$$

$$\frac{x_i}{D} \geqslant 12. \tag{21}$$

If (19) is not met, the firing is not intense any more and the similarity condition (12*a*) must be taken into account. For most of the firearms, (19) holds, and for this reason the source can be considered as a point source within the domain defined by (20) and (21).

4.4. *Effect of the temperature ratio*

Considering §4.2, we can replace (11*b*) by

$$\frac{\bar{T}}{T_g} = \frac{\bar{T}'}{T'_g}. \tag{22}$$

Yet, the parameter $\bar{T}/T_g$ is one of the most costly to adjust in a wind tunnel. We have seen elsewhere that T_g varies little from one kind of powder to another, so that the condition (22) is practically equivalent to $\bar{T} = \bar{T}'$. This means that, to make a wind-tunnel simulation of a shot at an altitude of 11000 m, the temperature in the tunnel test section must be 223 °K. So, from a practical point of view, it is essential to find if the effect of this parameter can be neglected.

To do this, all of the dimensionless parameters must be fixed while $\bar{T}/T_g$ is varied alone. We present in figure 12, results for two values of this parameter: 0.16 and 0.21. Since T_g is almost the same for all the guns studied, this comes down to varying $\bar{T}$ in the box. The technical difficulty stems from the fact that $\bar{c}$ occurs in each of the three parameters of the muzzle wave formation phase, i.e. M_p, $\mathscr{I}(L/D)$ and $\overline{p_T c}/p_g c_g$. We now place ourselves in the case where (19) is verified and where, in the domain defined by (20)–(21), the propagation is given by (24).

Figure 12 shows that the variation in the parameters $\mathscr{I}(L/D)$ and $\overline{p_T c}/p_g c_g$ induced by the variation in $\bar{c}$ has, in two different physical configurations, an imperceptible effect on the shape of the muzzle wave.

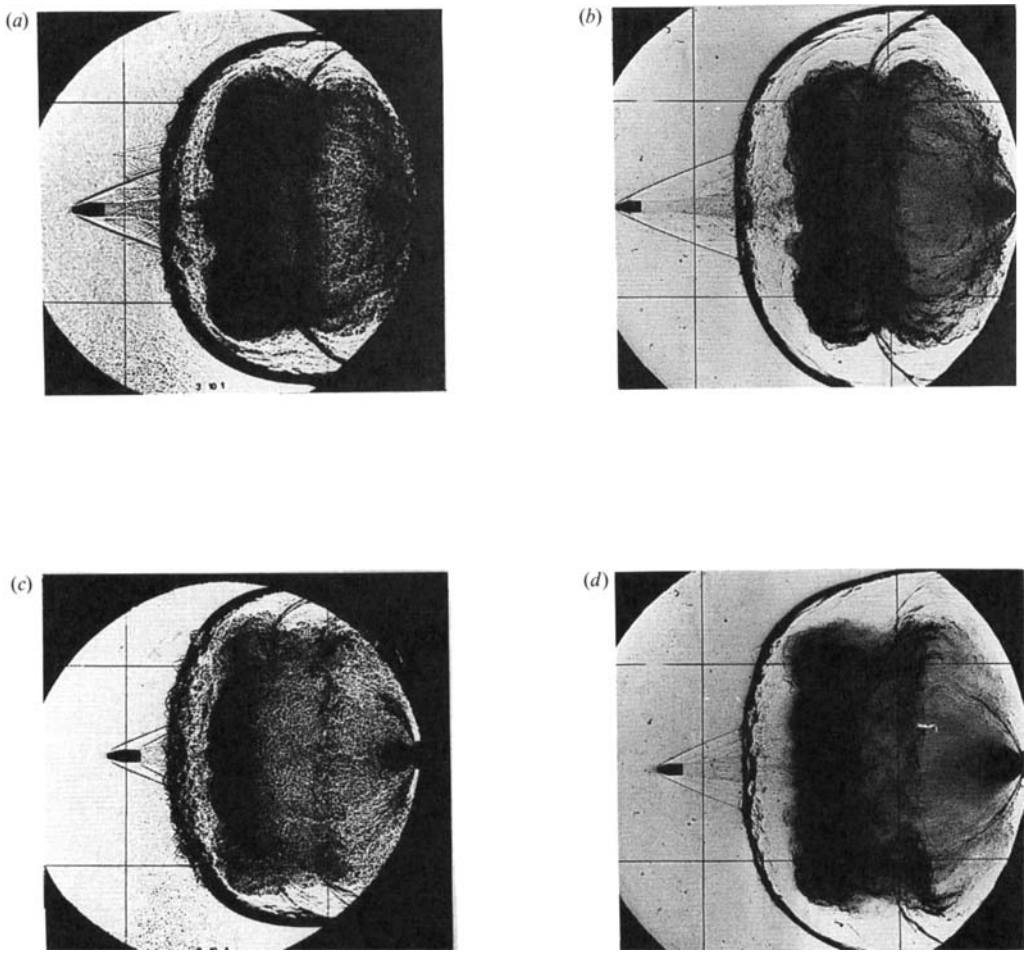

FIGURE 12. Blast waves for two values of $\bar{T}/T_g$. Photographs (*a*) and (*c*) correspond to $\bar{T}/T_g = 0.16$ ($\bar{T} = 223$ °K), photographs (*b*) and (*d*) to $\bar{T}/T_g = 0.21$ ($\bar{T} = 290$ °K). The value of M_p was the same in the four firings ($M_p = 3.38$), it was adjusted by choosing a lighter projectile for $\bar{T} = 290$ °K ($V_p = 1015$ m/s in (*a*)–(*b*); and 1150 m/s in (*b*)–(*d*)). The pressure $\bar{p}$ is 1 bar in firings (*a*) and (*b*) and 0.6 bar in (*c*) and (*d*). The small variation of $\mathscr{I}(L/D)$ and $(\bar{c}/c_g)/\overline{p_T}/p_g)$ induced by the modification of $\bar{c}$ has been tolerated ($\mathscr{I}(L/D)$ and $(\bar{c}/c_g)/(\overline{p_T}/p_g)$ were respectively 3.39 and 1.210^{-3} in (*a*) and 3.62 and 1.310^{-3} in (*b*); 2.63 and 0.710^{-3} in (*c*) and 2.8 and 0.810^{-3} in (*d*)). The other similarity conditions hold between (*a*) and (*b*) on the one hand and between (*c*) and (*d*) in the other. No effect on the shape of the waves is detected for a variation of $\bar{T}/T_g$.

The parameter M_p was held constant while V_p was modified. This is why a larger and slower projectile is seen in the photos taken at $\bar{T} = 223$ °K (figure 12).

The variation of $\bar{T}/T_g$ has no perceivable effect on the axial propagation (figure 13). This result remains valid for the other azimuth since $\bar{T}/T_g$ has no effect on the waveform. It is true that this result could be attributed to the small variation in the parameter. However, for applications, this interval of 0.16 to 0.2 covers the variation encountered by changing the altitude or the powder. So we can replace condition (22) by

$$0.16 \leqslant \frac{\bar{T}}{T_g} \leqslant 0.2. \tag{23}$$

This condition is very easily achieved, technically.

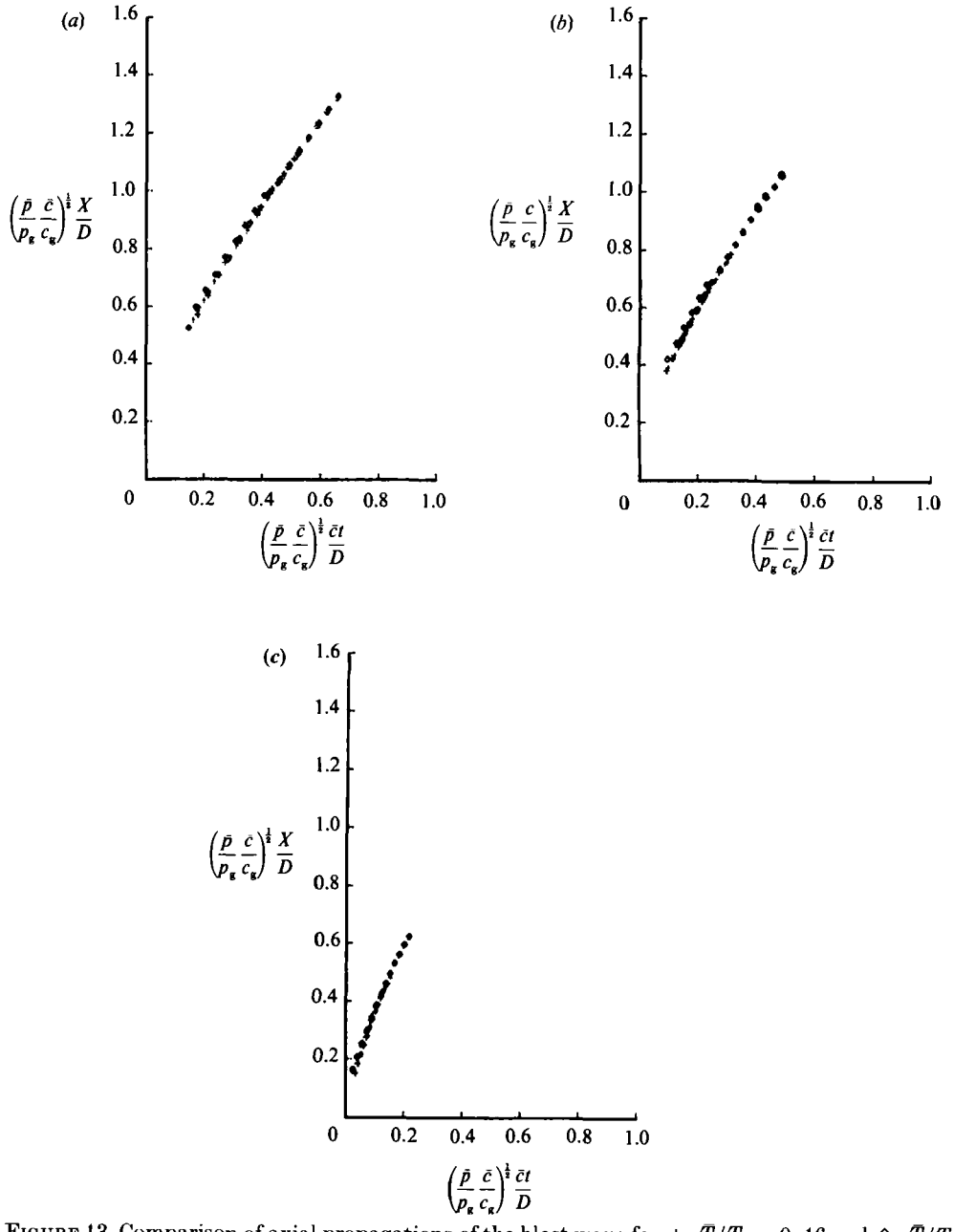

FIGURE 13. Comparison of axial propagations of the blast wave for +, $\bar{T}/T_g = 0$, 16 and ◇, $\bar{T}/T_g = 0$, 21. Graph (*a*) corresponds to firing (*a*) and (*b*) of figure 12, graph (*b*) to (*c*) and (*d*) of figure 12, graph (*c*) to the firing of the same weapon for $\bar{p} = 0.2$ bar. The range of $\bar{T}$ and $\bar{p}$ values is chosen to simulate the atmospheric variations between the altitudes $Z = 0$ and $Z = 11000$ m. No significant differences appear in any configuration.

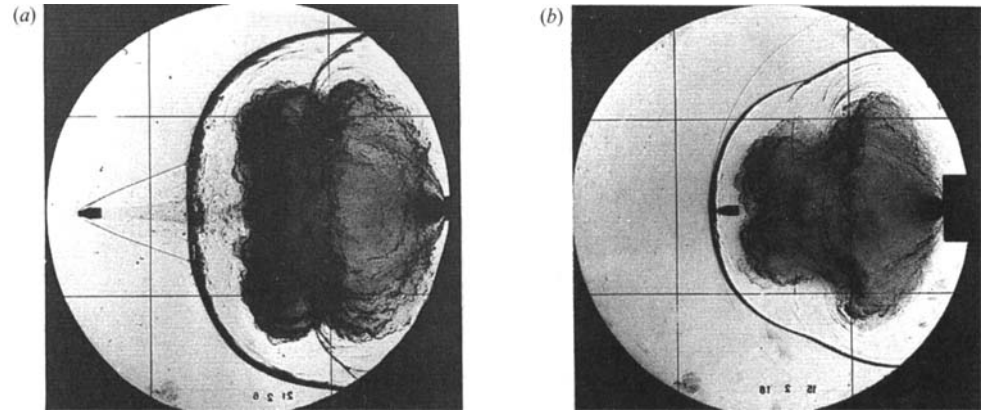

FIGURE 14. Blast waves for two values of M_p. Similarity conditions for intense firings hold except on M_p the variation of which is obtained by a smaller muzzle pressure p_g in (*b*): $M_p = 3.38$ in (*a*) and 2.26 in (*b*). $\mathscr{I}(L/D) = 2.44$ and $(\bar{c}/c_g)/\overline{p_T}/p_g) = 1.3^{-3}$ in both cases. The value of $\bar{T}$ was 290 °K and $\bar{p}$ was adjusted in order to maintain $\bar{p}/p_g$ constant. The effect of M_p on the shape of the wave has to be noticed.

By (19) and (23), we got around the conditions (11) and we can therefore write (16) in the form

$$\mathscr{I}\frac{X}{D} = \chi\left(\gamma, \gamma_g, M_g, \bar{M}, M_p, \mathscr{I}\frac{L}{D}, \frac{\overline{p_T c}}{p_g c_g}, \mathscr{I}\frac{\bar{c}t}{D}\right). \tag{24}$$

An important question is whether or not the conditions (19) and (23) are sufficient for the similarity to be verified for variables other than X in the domain defined by (20)–(21). We will deal with this problem experimentally for the pressure, in §5.1, and we will address it from the theoretical point of view in §6.

4.5. *Influence of the formation phase in an infinite atmosphere*

We have seen in §4.3 that, if we comply with (12), we get similar shapes of the muzzle waves for intense firing. Figure 14 shows that a major variation in M_p results in a modification of this geometric shape.

However, if we compare the physical configurations for $\bar{T} = 290$ °K of figure 12 and figure 15, we see that, despite the simultaneous variations of $\mathscr{I}L/D$ and $\overline{p_P c}/p_g c_g$, the shape of the wave is modified little.

In fact, in these tests, the variation of two parameters is a special case, because $\mathscr{I}(L/D)\,(\overline{p_T c}/p_g c_g)^{\frac{1}{2}}$ is constant. This suggests writing (12) in a form where the previous combination plays the role of an independent similarity parameter. We then get

$$\left(\frac{p}{p_T}\right)^{\frac{1}{2}}\frac{L}{D} = \left(\frac{\bar{p}'}{p'_T}\right)^{\frac{1}{2}}\frac{L'}{D'}, \quad M_p = M'_p, \quad \mathscr{I}\frac{L}{D} = \mathscr{I}'\frac{L'}{D'}. \tag{25a–c}$$

In (25), the first two conditions ensure that the geometries of the muzzle waves are identical for intense firing. The last condition is then found to be only a minor one, providing the similarity in the duration of the formation phase, but having no consequence on the shape or later propagation law of the wave.

This fortunate result for intense firing is illustrated by figure 16, showing that the precursors are not in similarity and that all this induces a simple time shift between the muzzle wave propagation curves. In order to illustrate the continuity of the slope we have suppressed this time shift on the second graph.

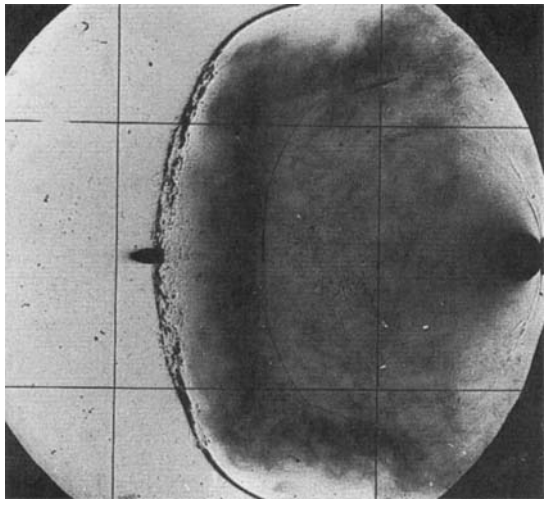

FIGURE 15. Blast wave of a 5.56 mm gun for $\bar{p} = 0.2$ bar. As in figure 12 (*b*) and (*d*) $\bar{T} = 290$ °K, $V_p = 1150$ m/s and $M_p = 3.38$. Parameters $\mathscr{I}(L/D)$ and $(\bar{c}/c_g)/\overline{p_T}/p_g)$ was 1.62 and 0.310^{-3}. Despite these much smaller values of $\mathscr{I}(L/D)$ and $(\bar{c}/c_g)/\overline{p_T}/p_g)$ than in figure 12 (*b*) and (*d*), the shape of the wave is almost the same. This fact happens probably because the parameters vary in such a manner that $\mathscr{I}(L/D)(\bar{c}/c_g)/\overline{p_T}/p_g)^{\frac{1}{2}}$ remains constant.

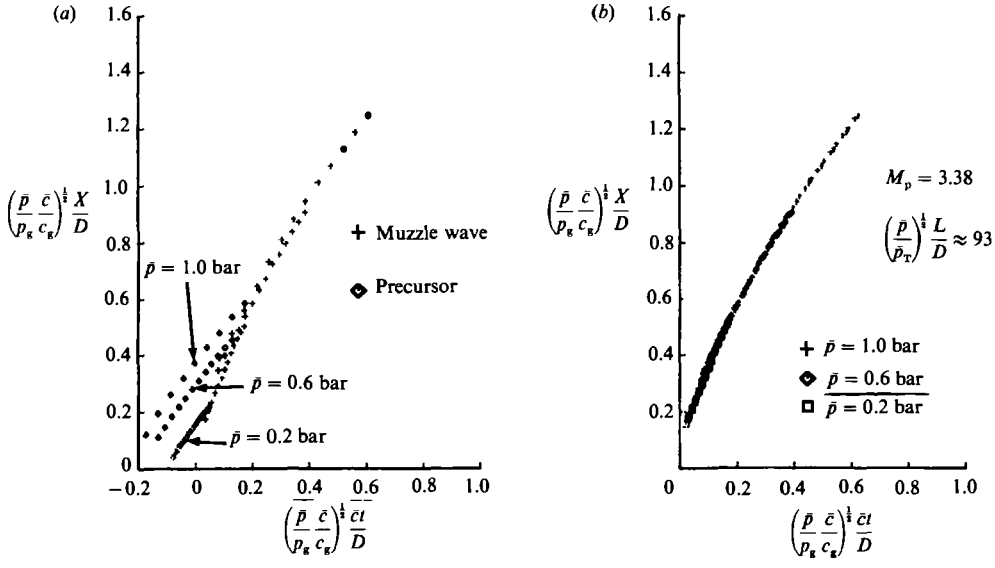

FIGURE 16. Effect of $\mathscr{I}(L/D)$ on axial propagation for different values of $\bar{p}$. Graph (*a*) shows that the precursors are not similar which induces a time shift between the muzzle wave propagation curve. Graph (*b*) shows the continuity of the propagation curve slopes by suppressing this time shift. $\mathscr{I}(T/D)$ is equal to 1.62, 2.8, 3.4 respectively for $\bar{p} = 0.2$, 0.6 and 1 bar.

Technically the conditions (25.1) and (25.2) are easily attainable, and the fact that (25.3) is not strictly complied with if we allow the initial time shift, brings in an additional freedom: the simulation gun does not necessarily have to be in geometric similarity with the simulated gun i.e. L/D and L'/D' can be different. Moreover, thanks to (25*a*) and (25*b*), we can simulate any range of waveforms, including that of a gun with two precursors.

Of course, further experiments can be done to determine, for example, the influence of $\mathscr{I}$ on the shape of the wave at the beginning of its propagation, but, for practical applications involving intense firings in the presence of a body, conditions (25) are of less importance in the domain defined by (20) and (21).

5. Practical application of similarity

5.1. *Firing in the presence of a body*

There are many advantages to firing a downscale firearm that is similar to a large- or medium-calibre gun, particularly when we want to study the effect of the blast wave on the surrounding structures or on the outer flow. If the body is far enough from the muzzle for the wave to form as it would in an infinite atmosphere, the above analysis remains valid. The body is then characterized by a length H giving the additional condition

$$\mathscr{I}\frac{H}{D} = \mathscr{I}'\frac{H'}{D'}. \tag{26}$$

H and D are related only by (26) because the conditions (19), (23), (25a) and the tolerance on (25c) allow us to separate the three lengths L, H and D involved in the problem into independent entities. So we do not need to choose the same scale to reduce the model and the calibre. This way, we can use a standard gun and change the loading conditions to obtain a broad range of simulated cases, and can then choose another calibre or another scale of model to enlarge the domain being explored, though the body must remain in the domain defined by (20) and (21).

The question that arises then is: what happens when the interaction between the body and the shot begins right at the formation phase and in the vicinity of the muzzle?

Experiments bring a satisfactory answer to this question. In fact, it happens that the presence of the body modifies the shape of the muzzle wave considerably and, if the interaction occurs very early in the development of the jet of burned gases, the conditions (25) no longer have any more than a minor effect on the shape of the wave (figure 17).

We see that if $\overline{p_T}$ is small (second case in figure 20), the wave behaves like an ideal firing. This is true for shots fired at high altitude.

In the presence of a body, p can be measured in addition to X. Concerning such experiments, the most probative one in our opinion was to use a 5.56 mm rifle to simulate a 30 mm gun placed in a gutter and in the presence of a simplified fuselage (figure 18).

All of the conditions of (10), in which $\overline{M} = 0$, (25), (19) and (26) are met.

Figure 19 shows the dimensionless pressure signals obtained on the transducer indicated by an arrow in figure 18. The similarity is not achieved over the length of the projectile, which is shorter for the rifle. This explains the difference on the location of the first pressure peak which corresponds to the wave attached to the projectile nose. This wave seems to be almost as strong as the blast wave because the transducer has been set close to the firing axis. Actually, the decay of this attached wave is very quick and the blast wave is not modified.

The signals cannot be made perfectly identical because the transducers and their passband are not similar for obvious technical reasons. Moreover, in the case of the rifle, the box walls create parasitic reflections.

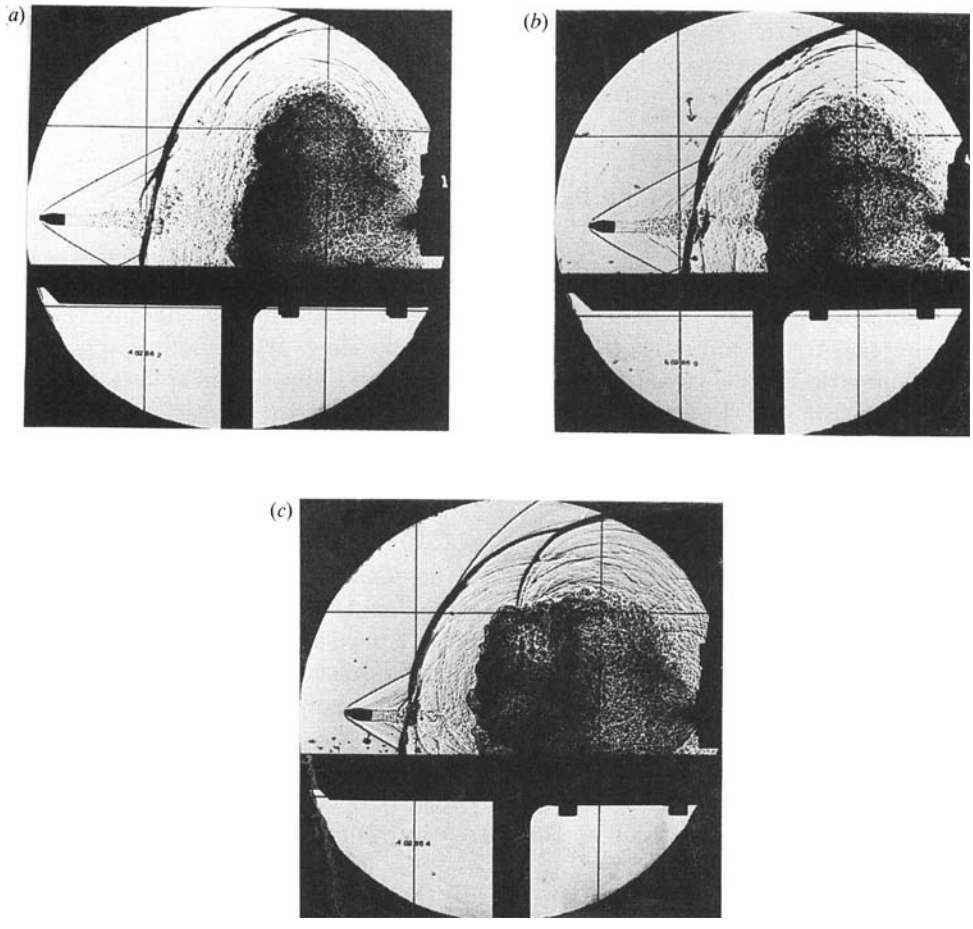

FIGURE 17. Shape of blast waves in presence of a body. (*a*) is an ideal firing, (*b*) and (*c*) firings with a formation phase ($M_p = 2.4$, $\mathscr{I}(L/D) = 5.3$). In firing (*c*), $(\bar{c}/c_g)/\overline{p_T}/p_g) = 2.910^{-3}$ and the formation phase was stronger than in (*b*) for which a membrane has been used in order to reduce $\bar{p}_T$ and to obtain: $(\bar{c}/c_g)/\overline{p_T}/p_g) = 0.310^{-3}$. Despite of this different formation phases, the shapes of the waves are very similar, particularly in the vicinity of the body.

The measurement in figure 19 may correspond to what happens at the lip of an air intake. So we can use the shooting similarity defined above to study problems of interference between the shooting of the aircraft guns and engine operation.

5.2. *Application to the problem of firing-air intake interference*

In the presence of an air intake, the mass flow rate Q_m in the engine must be added to the characteristic parameters of the phenomenon. By applying our adimensionalization, we arrive at the new similarity condition

$$C_q = C'_q, \tag{27}$$

in which

$$C_q = \frac{Q_m}{\bar{\rho}\bar{U}\mathscr{A}}$$

is the mass flow rate coefficient and $\mathscr{A}$ the characteristic area of the air intake related to H by $\mathscr{A}/H^2 = cst.$

(*a*)

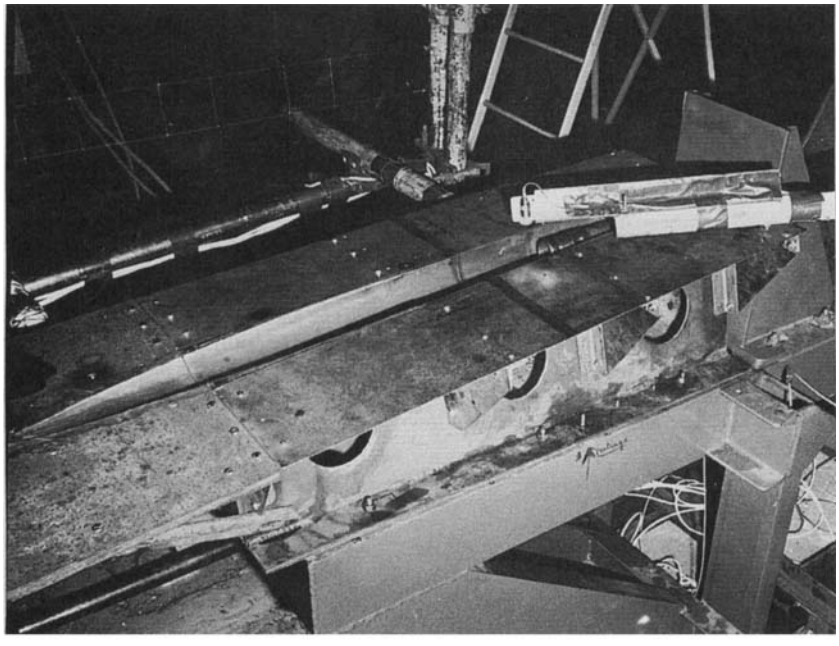

(*b*)

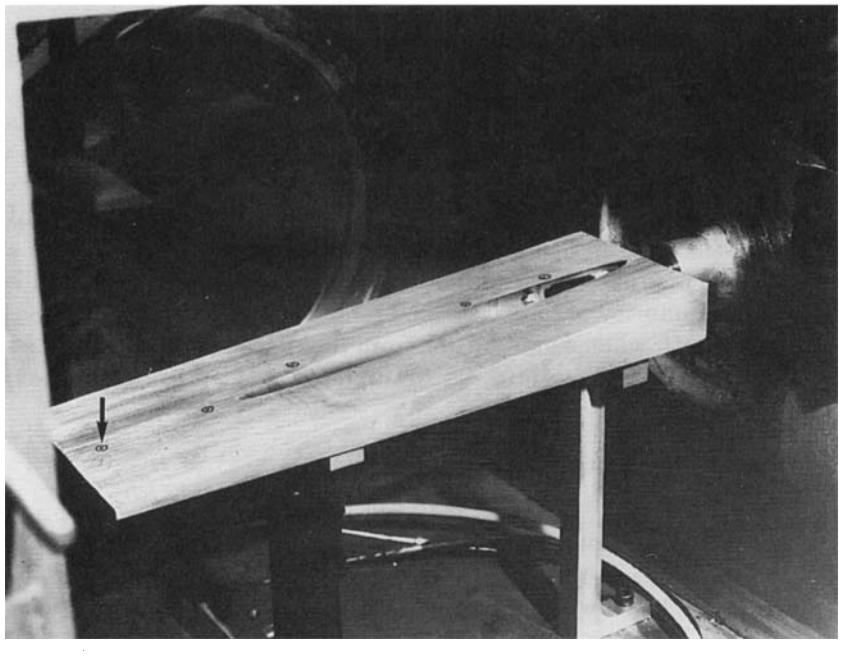

FIGURE 18. Partial view of the 30 mm gun firing facility (*a*) and its small scale model (*b*). The arrow on (*b*) gives the location of the pressure transducer the measurement of which is presented in figure 19.

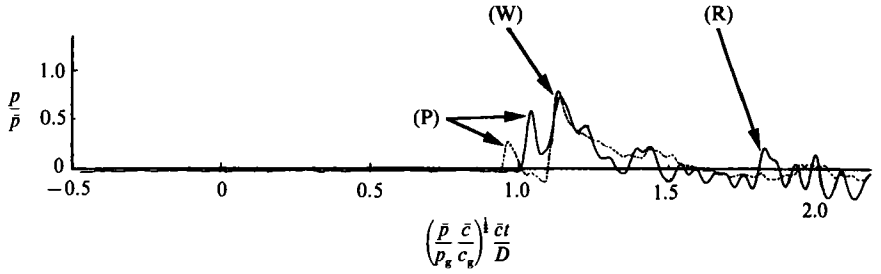

FIGURE 19. Pressure measurements comparison between —, the cannon and - - -, the 5.56 mm similar gun. The dimensionless pressures on the front of the blast waves (W) are identical, but the waves associated to the projectile (P) are not similar. The same kind of transducer is used in both cases, so the passbands and the membrane size of the transducers are not adjusted according to the similarity: consequently, oscillations can be noticed on the gun signal but not on the cannon one. The reflection on the box walls (R) does not allow the comparison when the dimensionless time is greater than 1.75.

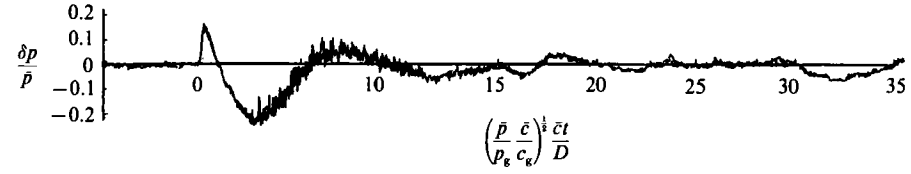

FIGURE 20. Pressure measurement inside the air intake at a distance from the inlet plane corresponding to the engine position. It can be noticed that the oscillations of the signal last much longer than the muzzle wave phenomenon.

Wind-tunnel tests have been conducted on a simplified air intake consisting of a cylindrical duct set at an angle of attack.

Figure 20 gives an example of a measurement recorded by a pressure transducer placed perpendicular to the air intake cross-section and at a distance from the inlet plane that could correspond to the engine position (i.e. about $8\mathscr{A}^{\frac{1}{2}}$).

Finally, thanks to the similarity, we have arrived at a viable experimental method for studying problems of gun firing-air intake interference. This provides a wealth of information for the manufacturers of both the aircraft and the engine. Of course, it is obvious that the quantity of data obtained on a model in wind-tunnel tests cannot even be compared with what would be got from flight tests, where visualizations are impossible and where configurations are limited, for cost and safety reasons.

6. Interpretation and modelling

6.1. *Point source of hot gases*

In the case of an intense shot, experience suggests that we could simplify things by assimilating the gun muzzle to a finite point source of mass, momentum and energy as we have seen in §4.3. We will appraise now the consequences this approach has on a theoretical level. The flow rates (1) are characterized by $\mathscr{Q}$, $p_g D^2$ and $\mathscr{P}$. The hypothesis that the burned gases constitute an ideal gas means that

$$\mathscr{Q} \sim \rho_g c_g D^2,$$
$$p_g D^2 \sim \rho_g c_g^2 D^2,$$
$$\mathscr{P} \sim \rho_g c_g^3 D^2.$$

Let us suppose that D tends toward zero. The quantities $\mathscr{Q}$, $p_g D^2$ and $\mathscr{P}$ remain finite if c_g or ρ_g tends toward infinity. Speaking of a gas, it is physically absurd to consider ρ_g as infinite; so it remains to be assumed that c_g becomes infinite. If this is the case, all three quantities considered may remain finite only if

$$c_g \sim \frac{1}{D^{\frac{2}{3}}},$$

in which case $\mathscr{Q}$ and $p_g D^2$ tend toward zero. So, we can conclude that by idealizing the muzzle to a point source we must necessarily consider the burned gases as being infinitely hot and the added mass and momentum as being negligible.

The intense shot is then likened to a point source adding energy at a constant rate into a compressible medium. This is a special case of the problem of a point explosion in a gas, which has been dealt with abundantly in the scientific literature. The case of the isotropic point explosion with instantaneous addition of energy has served as a model for atomic explosions (Taylor 1950; Sedov 1945; Sakuraï 1965). The case of an isotropic addition of energy of the form $\mathscr{E} = Et^\alpha$ has been used, among other things, for modelling the effect of a strong electric discharge of cylindrical symmetry (Freeman 1968) or, by way of analogy of the equations, to calculate hypersonic cylindrical or planar flows. However, no application has been found to the case of the point explosion (spherical case) when the energy is not added instantaneously. We can see here that this concept is suitable for the intense firing.

Before going any further with the modelling, we should return to the physical interpretation of the shot. Since we have likened the gun muzzle to a point source, the intense shot can be produced only by a very hot gas, in which case $\bar{T}/T_g$ is a small parameter that is not independent of $\mathscr{I}$ since ρ_g remains infinite. If one tends toward zero, the other must be considered as zero too. That means that the simplifications obtained in §§4.3 and 4.4 derive from each other. From this fact, we can replace (25) by:

$$0 < \frac{\bar{T}}{T_g} \leqslant 0.2. \tag{28}$$

The developments in this section clearly show that the choice of $\mathscr{P}$ as a primary quantity is the only one which allows the simplifications made in §§4.3 and 4.4. We can illustrate this remark as follows.

To simplify the notation, let us take the case of the ideal firing in an infinite atmosphere at rest. We have

$$\mathscr{I}\frac{X}{D} = \chi_D\left(\gamma, \gamma_g, M_g, \frac{\bar{c}^2}{c_g^2}, \mathscr{I}, \mathscr{I}\frac{\bar{c}t}{D}\right). \tag{29}$$

In the domain defined by (20) and (21) with the intense shot hypothesis, we arrive at

$$\mathscr{I}\frac{X}{D} = \chi_0\left(\gamma, \gamma_g, M_g, \mathscr{I}\frac{\bar{c}t}{D}\right). \tag{30}$$

Yet, it is possible to go to the limit like this only if $p_g c_g D^2$ remains finite; otherwise the variables would not be independent and (30) would be valid only for zero X and t. This means that the function χ_0 is actually an asymptotic limit of the first type for χ_D (Barenblatt 1979).

If we had chosen $p_g D^2$ as a primary quantity instead of $\mathscr{P}$, we would have written:

$$\left(\frac{\bar{p}}{p_g}\right)^{\frac{1}{3}}\frac{X}{D} = \tilde{\chi}_D\left(\gamma, \gamma_g, M_g, \frac{\bar{c}}{c_g}, \left(\frac{\bar{p}}{p_g}\right)^{\frac{1}{2}}, \left(\frac{\bar{p}}{p_g}\right)^{\frac{1}{3}}\frac{\bar{c}t}{D}\right). \tag{31}$$

This formula is equivalent to (29) and leads to the same similarity conditions. If we assume that there exists a limit $\tilde{\chi}_0$ of the first type of $\tilde{\chi}_D$ when $\bar{c}/c_g$ tends to zero, we get

$$\left(\frac{\bar{p}}{p_g}\right)^{\frac{1}{3}}\frac{X}{D} = \tilde{\chi}_0\left(\gamma, \gamma_g, M_g, \left(\frac{\bar{p}}{p_g}\right)^{\frac{1}{2}}, \left(\frac{\bar{p}}{p_g}\right)^{\frac{1}{3}}\frac{\bar{c}t}{D}\right). \tag{32}$$

This form is no longer equivalent to (30) because it is founded on the hypothesis that $p_g D^2$ remains finite if D tends toward zero, i.e. that $\mathscr{P}$ tends towards infinity. We then no longer have a physically acceptable model and there is no justification for going to the limit.

In fact, χ_0 corresponds to an asymptotic limit of the second type for $\tilde{\chi}_D$, such that $(p/p_g)^{\frac{1}{3}}X/D$ tends toward infinity as $(\bar{c}/c_g)^{-\frac{1}{2}}$ when $\bar{c}/c_g$ tends toward zero.

In more physical terms, we may say that going to the limit for $\bar{c}/c_g$ tending toward zero does not have the same meaning in (30) as it does in (32). In (32), it assumes that a variation of T_g and therefore of the three flow rates at the muzzle, has no effect on the propagation of the muzzle wave, which is absurd since that comes down to saying that the effect is independent of the cause. In (30), on the other hand, it means that for a hot jet the variations of the mass flow rate alone have no consequence if the energy added is constant.

To obtain this physical model of the intense firing, we proceeded by inductive reasoning, starting from an experimental observation, and giving it a theoretical interpretation. To validate this concept, we must now use the model to predict a physical behaviour of the muzzle wave, which we will be able to verify experimentally.

6.2. *Experimental confirmation of the model*

As is frequently done in strong shock waves studies (Sedov 1959), we now suppose that the influence of $\bar{p}$ is negligible. Necessarily the formula (30) must remain a finite combination of X and t independent of $\bar{p}$. The only possible form is therefore:

$$X = K(\gamma, \gamma_g, M_g)\left(\frac{\mathscr{P}}{\bar{\rho}}\right)^{\frac{1}{5}} t^{\frac{3}{5}}.$$

In this expression, $\bar{p}$ no longer appears. As in the instantaneous explosion problem treated by Sedov (1945) and Taylor (1950), there remain only two dimensional constants, $\mathscr{P}$ and $\bar{\rho}$. Consequently, we are in the presence of a self-similar problem in which t can act as a primary quantity.

Experimentally, the expression (30) is valid only in the domain defined by (20)–(21). This means that there exists an uncertainty concerning the time origin and the position of the point source to which we liken the shot. In a frame centred on the muzzle, we assume here that this position (X_0, t_0) exists and is given by a formula of the form

$$X_0 = f\left(\frac{\bar{c}^2}{c_g^2}, \mathscr{I}\right)D, \quad t_0 = g\left(\frac{\bar{c}^2}{c_g^2}, \mathscr{I}\right)\frac{D}{\bar{c}},$$

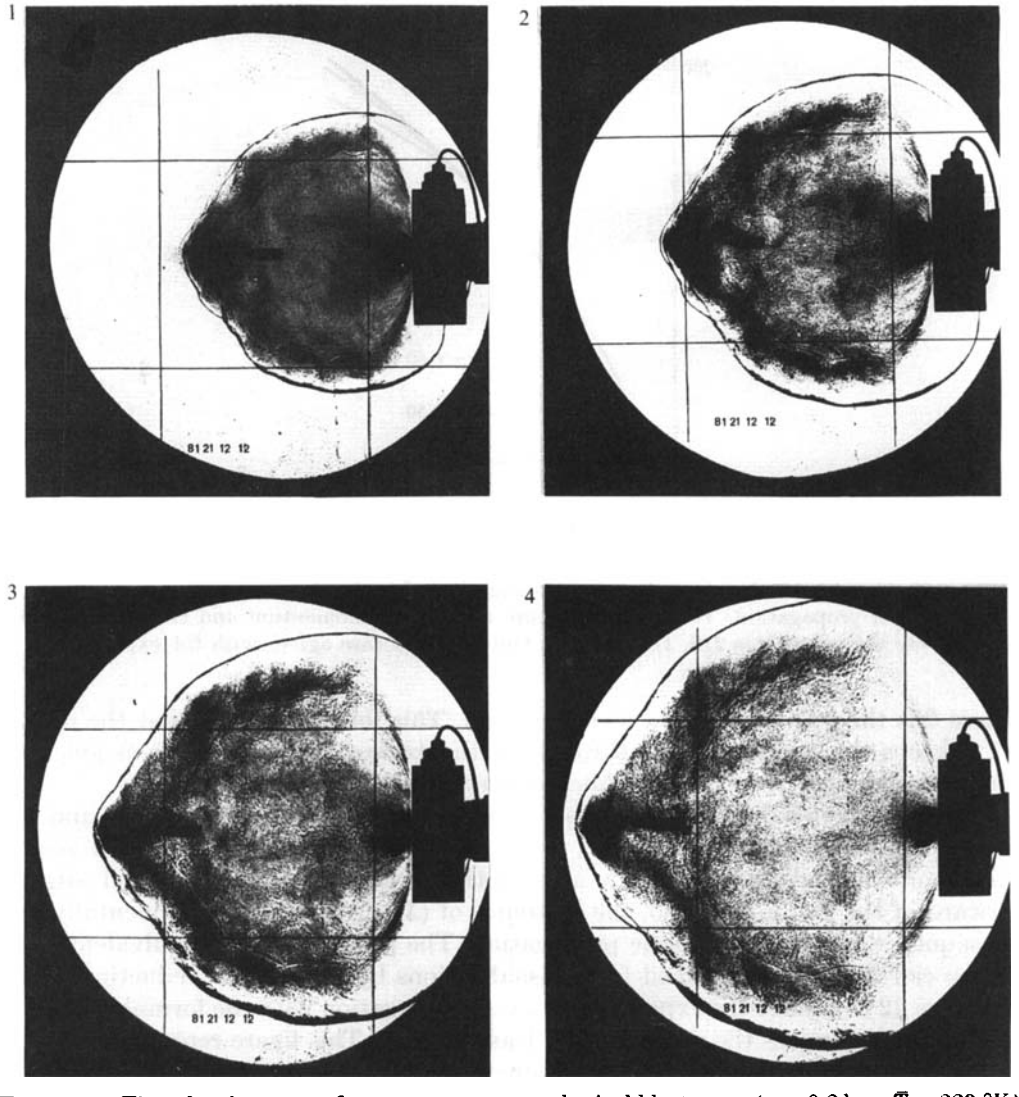

FIGURE 21. Time development of a very strong non-spherical blast wave ($\bar{p} = 0.2$ bar, $\bar{T} = 223$ °K). The time interval between photographs is $\Delta t = 20$ μs. The numbers indicate the sequential order. The successive position of the wave does not vary with time. Each position of the wave can be deduced one from another by a homothetic dilatation the centre of which is situated at a distance of about three calibres forward the muzzle.

in which the functions f and g are of the order of unity. If $\bar{p}$ is negligible, we can then expect the shock to propagate axially according to

$$X - X_0 = K\left[\frac{\mathscr{P}}{\rho}(t-t_0)^3\right]^{\frac{1}{5}}. \tag{33}$$

More generally, by placing the origin at the abscissa point X_0, we can write the position of the shock in the form

$$R(t, \theta) = R_0(\gamma, \gamma_g, M_g, \theta)\left[\frac{\mathscr{P}}{\rho}(t-t_0)^3\right]^{\frac{1}{5}}$$

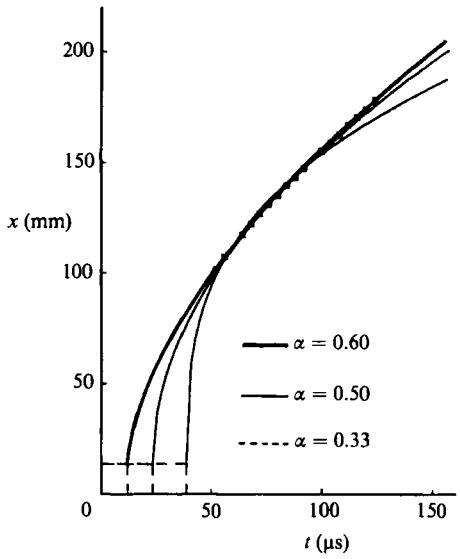

FIGURE 22. Comparison between the axial propagation of an intense blast wave and self similar power laws of propagation. To a source of pure mass, pure momentum and energy correspond respectively the values $\alpha = 2/3$, $1/2$ and $3/5$. Only the last case agrees with the experiments.

where θ is the polar angle in a meridian plan. This formula means that the muzzle wave keeps the same geometry throughout the expansion, and does so as long as $\bar{p}$ remains negligible, i.e. that the shock is very intense.

Figure 21 shows that this is actually the case when the shot is intense and $\bar{p}$ is small. We observe that the wave, made anisotropic by the effect of a second precursor, expands according to a homothetic transformation centred slightly forward of the gun muzzle. So, the existence of (X_0, t_0) appears experimentally as a consequence of that homothetic propagation. The position of that equivalent point source can then be determined from visualizations by homothetic reduction.

Figure 22 compares the experimental axial propagation with the formula (33). The calculation optimizes the value of t_0 by least squares. This figure represents also the propagations that would exist with a source of pure momentum and a source of pure mass, i.e. when the jet of burned gases is characterized respectively by $p_g D^2$ and $\mathscr{Q}$ instead of $\mathscr{P}$. For this two cases, dimensional analysis also leads to power law propagations $R = K(t-t_0)^\alpha$, with $\alpha = 1/2$ for a source of pure momentum and $\alpha = 2/3$ for a source of pure mass. It is clear that these two sources cannot represent any physical reality, so it is no surprise that they are not in accordance with the experimental values.

The experiment therefore shows that likening the intense shot to a finite point explosion with constant rate of added energy is in conformity with reality, at least as far as the shock propagation is concerned. So we have found a theoretical equivalence of the gun firing that is simple enough to be usable for calculations. If we find a solution to this theoretical problem, we will have proved the existence of the function χ_0 for a point source; but the greatest advantage of such a calculation is that it gives a way of determining quantities that are not measurable. It will then be possible to discuss the value of the point source hypothesis according to which $\mathscr{Q}$ is zero, and we may hope that this will help us understand why $\mathscr{Q}$ has so little effect on X and p.

We see here that the advantage of the model goes beyond the framework of its application to the firearm, and that it deserves a discussion of its own. However, to suit the shooting configuration, the explosion model cannot be limited to the self-similar base flow, because this concerns only very intense shoots. So it seems that the theory must be made usable for weaker shocks, and must therefore take the effect of $\bar{p}$ into account. In the final analysis, two lines of research might be adopted in view of applying the model to the firing of aircraft guns. The first concerns the effect the anisotropy of the added energy has, because it is evident that the jet of burned gases is not an isotropic source. The second concerns the effect of the oncoming flow.

7. Conclusion

On the basis of precise experimental observations, chiefly ultra-high-speed visualizations, we have been able to carry out a detailed phenomenological analysis of the discharge of firearms. We have isolated the essential aspects and have applied a method of analysis based on the theory of similarity.

On the applications level, we have arrived at the definition of the conditions governing the tests on models. We can summarize these as follows.

Base conditions:

$$\gamma = \gamma', \quad \gamma_g = \gamma'_g, \quad \bar{M} = \bar{M}', \quad M_g = M'_g = 1;$$

Body related conditions:

$$\left(\frac{\bar{p}}{p_g}\right)^{\frac{1}{3}}\left(\frac{\bar{c}}{c_g}\right)^{\frac{1}{3}}\frac{H}{D} = \left(\frac{\bar{p}'}{p'_g}\right)^{\frac{1}{3}}\left(\frac{\bar{c}'}{c'_g}\right)^{\frac{1}{3}}\frac{H'}{D'}, \quad C_q = C'_q;$$

Waveform related conditions:

$$\left(\frac{\bar{p}}{p_T}\right)^{\frac{1}{3}}\frac{L}{D} = \left(\frac{\bar{p}'}{p'_T}\right)^{\frac{1}{3}}\frac{L'}{D'}, \quad M_p \simeq M'_p;$$

Order of magnitude conditions:

$$\left(\frac{\bar{p}}{p_g}\right)^{\frac{1}{3}}\left(\frac{\bar{c}}{c_g}\right)^{\frac{1}{3}}\frac{L}{D} \sim \left(\frac{\bar{p}'}{p'_g}\right)^{\frac{1}{3}}\left(\frac{\bar{c}'}{c'_g}\right)^{\frac{1}{3}}\frac{L'}{D'},$$

$$0 < \frac{\bar{T}}{T_g}, \quad \frac{\bar{T}'}{T'_g} \leqslant 0.2,$$

$$\left(\frac{\bar{p}}{p_g}\right)^{\frac{1}{3}}\left(\frac{\bar{c}}{c_g}\right)^{\frac{1}{2}}, \quad \left(\frac{\bar{p}'}{p'_g}\right)^{\frac{1}{3}}\left(\frac{\bar{c}'}{c'_g}\right)^{\frac{1}{2}} \leqslant 5 \times 10^{-2}.$$

These rules apply only in a domain defined by:

$$\frac{x_i}{D} \geqslant 12, \quad \frac{\bar{c}t}{D} \geqslant 5.$$

Experience shows that these rules suffice for representing the muzzle wave propagation and unsteady pressures on a reduced scale. They do not, however, impose similarity on the quantity of burned gases release.

Consequently, they apply only to practical problems where the blast effect predominates. This drawback is offset by the great ease with which tests can be run on models: no geometric similarity is required between the simulation gun and the

simulated one, and even the scales of the model and the simulation gun can be different. We can therefore use a standard gun and still cover a broad range of configurations by varying the ammunition or the scale of the model.

On the theoretical level, we have shown that the blast effect comes under the more general heading of intense explosions, and calls for several lines of further research, namely into the anisotropy of the source and the effects of the counter pressure $\bar{p}$ and of the external counterflow $\bar{U}$. It is in this direction that we are continuing our subsequent research on gun firing.

This research has been supported by the French Ministry of Defence, (DRET, G.6).

REFERENCES

BARENBLATT, G. I. 1979 *Similarity, self-similarity and intermediate asymptotics.* Consultants bureau. New York and London.

DYMENT, A. & MERLEN, A. 1981 Gun firing similarity for aircraft interference problems. *J. Aircraft* **18** (5), 415–416.

EICHHORN, A., WERNER, U., MACH, H. & MAZUR, H. 1984 Mesure des variations de la température en fonction du temps dans des écoulements de révolution. *ISL Rep. no.* 132/84.

FREEMAN, R. A. 1968 Variable-energy blast waves. *Brit. J. Appl. Phys.* Ser. 2, **1**.

FULLER, P. 1980 Measurement of bore yaw of projectiles. In *5th Int Symp. of ballistics*, Toulouse.

MACH, H. 1978 Mesure de la température et de la vitesse des gaz de combustion dans le tube et à la bouche d'une arme. *ISL Rep. No.* CO206/78.

MACH, H., KLINGENBERG, G., WERNER, U., MAZUR. H. & WEILAND, O. 1977 Mesure spectroscopique de la température des produits de combustion dans le tube et à la sortie de la bouche d'un canon automatique de 20 mm de calibre. *ISL Rep. No.* 106/77.

MERLEN, A. 1988 Similitude physique et modélisation par explosion équivalente des phénomènes aérodynamiques de balistique intermédiaire. Thèse de Doctorat d'Etat, Université des Sciences et Techniques de Lille Flandres Artois.

MERLEN, A. & DESSE, J . M. 1983 Similitude de tir, effet de la phase de formation, influence d'un obstacle. *IMFL Rep.* 83/64.

OSWATITSCH, K. 1964 *Zwischenballistik.* Deutsche Luft und Raumfahrt. DVL.

SAKURAÏ, A. 1965 *Blast Wave Theory. Basic Developments in Fluid Dynamics*, vol. 1. Academic.

SCHMIDT, E., GION, E. & FANSLER, K. 1980 Analysis of weapon parameters controlling the muzzle blast flow field. In *5th Intl Symp. of Ballistics, Toulouse.*

SCHMIDT, E. & SHEAR, D. 1975 Optical measurements of muzzle blast. *AIAA J.* **13**, 1086–1091.

SEDOV, L. I. 1945 On certain unsteady compressible fluid motions. *Appl. Maths Mech. Leningr.* **9** (4), 294.

SEDOV, L. I. 1959 *Similarity and Dimensional Methods in Mechanics.* Academic.

TAVERNIER, P. 1954 Balistique intérieure. *Mémorial de l'Artillerie Française*, fasc. 3–4, pp. 623–866.

TAYLOR, G. I. 1950 The formation of a blast wave by a very intense explosion. *Proc. R. Soc., Lond.* **A201**, 159–66.